

2002, Volume 8

ISSN 1024-669X



# HONG KONG GEOLOGIST

*The Journal of the  
Geological Society of Hong Kong*

# HONG KONG GEOLOGIST

## *The Journal of the Geological Society of Hong Kong*

This journal publishes research articles, short communications and reviews related to Hong Kong, Macau and the South China region. It incorporates the previously published Newsletter of the Geological Society of Hong Kong.

The Geological Society of Hong Kong is primarily concerned with the study and dissemination of geologic knowledge and the advancement of the geologic sciences within Hong Kong and the surrounding regions.

*Articles and Short Communications:* Manuscripts for publication should be submitted in English to the Editor as follows: one hard copy (double spaced, on one side of the paper only) and one disc copy (IBM compatible). Pagemaker 6.5 and Microsoft Word are the preferred word processing formats, though all common word processing packages are acceptable.

Original line drawings (not photocopies) should be submitted on separate sheets and be suitable for reproduction in either a two-column format (maximum width of 155 mm) or single-column format (maximum width of 75 mm). Half-tone illustrations (preferably as good glossy bromide prints) should be suitable for reproduction in the same manner. The maximum page depth is 235 mm. Where figures are available on disc, they should be submitted as both hard copy and disc copy.

The format of the manuscripts should follow that used in this issue of Hong Kong Geologist.

All research papers are refereed and the journal assumes that all authors of a multi-authored paper agree to its submission.

The language of the journal is English, though Chinese abstracts are also provided.

*Books for review.* Books for review should be addressed to the Editor. Preference will be given to those dealing with Hong Kong and its surrounding region, or with the methods, nature and study of the geological sciences.

*Advertisements.* Advertisements will be accepted for publication in the Hong Kong Geologist at the discretion of the Editor, in camera ready form only. The 1999 advertising rates are \$US 60 full page and \$US 30 half page.

*Editor:* Dr. R.B. Owen, Department of Geography, Hong Kong Baptist University, Kowloon Tong  
Tel: (852) 34117188,  
Fax: (852) 34115690,  
e.mail: owen@hkbu.edu.hk

*Issued:* annually

*Subscriptions:* Individual and institutional subscriptions are via membership of the Society, information on which can be obtained from:

Mr. Chow, Chun Hung (GSHK Secretary), c/o Dept. Earth Sciences, University of Hong Kong, Pokfulam Road

Students, \$HK 50 annually  
Full members, \$HK 200 annually  
Institutions, \$HK 250 annually

Overseas subscribers receive their issues by sea mail.



# Spatial Variation of Sediment Components in the Marine Deposits of Hong Kong

R.B. Owen

Department of Geography, Hong Kong Baptist University, Kowloon Tong, Hong Kong.

## Abstract

The continental shelf of Hong Kong is generally less than 25 m deep and is characterised by an extensive blanket of marine mud, interrupted locally by sandier deposits associated with tidal channels and areas exposed to high wave energy. The mud blanket is often considered to be uniform in its sedimentology. However, this study has shown that there are distinct, though often subtle, variations in composition and sedimentation rates. Organic matter ranges between 2 and 32%, with most samples containing between 5 and 15%. Carbonate generally comprises 2-25% of the mud, though local coquinas also occur. Biogenic silica is a minor component, with diatoms and sponge spicules dominating. Species diversity and abundance show clear spatial variation. Particle size trends are subtle but distinct. Sedimentation rates reported here range between 0.17 and 0.51 cm/a. Attempts to date sediments failed in western Hong Kong, possibly because of bioturbation effects.

## 摘要

香港沿岸的大陸架一般少於 25 米深，架上被大量海泥覆蓋，只有在潮汐通道或受能量高波浪影響的地區才間中有沙質沉積物。從沉積物學的觀點而言，覆蓋在大陸架上的海泥沉積規律變化不大。但這個研究發現，沉積物的成份及沉積率展示明難以察覺的差異。沉積物中有機物成份約在 2-32%之間；而大部份樣本則在 5-15%之間。海泥中的碳酸鹽含量約在 2-15%之間，間中亦發現有貝殼類物質。此外，海泥中亦發現少量含有硅藻及海綿的生源硅。這些生物的種類及數量有明顯的空間差異，顆粒大小變化不大但很突出其沉積率在每年 0.17 至 0.51 厘米之間。可能受到生物渾濁效應的影響，在香港西部地區收集的沉積物未能通過年份檢定。

## Introduction

Hong Kong lies on the southern coast of China (Fig. 1) and is about 1000 km<sup>2</sup> in land area, with a further 1000 km<sup>2</sup> of marine territory. The SAR is characterised by a variety of transitional environmental situations. It lies on the edge of the subtropics, experiencing hot wet summers and cold dry winters that are more typical of temperate locations. It lies at the boundary between land and sea and has a complex coastline that reflects early Holocene flooding of ancient river valley systems.

The modern marine environment exhibits a marked change from the turbid and brackish Pearl River Estuary in the west, through a transition zone in central areas, to the fully marine, low-turbidity, waters of eastern Hong Kong (Fig. 1, Inset C; Morton and Wu, 1974). Depth averaged turbidity values in the western (estuarine) sector range between about 6 and 110 NTU,

with secchi disc depths of about 0.2-1.5 m (Lam, 1994). Depth averaged suspended solids vary between about 20 and >250 mg/l (Parry, 2000). In contrast, the eastern oceanic sector typically shows turbidity values of about 2-10 NTU, secchi depths of 2-8 m, and suspended solid values of 1-10 mg/l (Lam, 1994). Parry (2000) notes the passing impact of Typhoon Sibyl in October 1995 near Po Toi Island (Fig. 1), with suspended sediments rising from a background level of 20 mg/l to >350 mg/l.

Marine sedimentation is controlled by four major factors (Fyfe *et al.*, 2000) that include freshwater outflow from the Pearl River, tidal regime, coastal currents, and in recent decades human impacts. The three natural controls, in turn, vary seasonally in response to changing rainfall, wind and temperature patterns. The Pearl River discharges 80 million tons

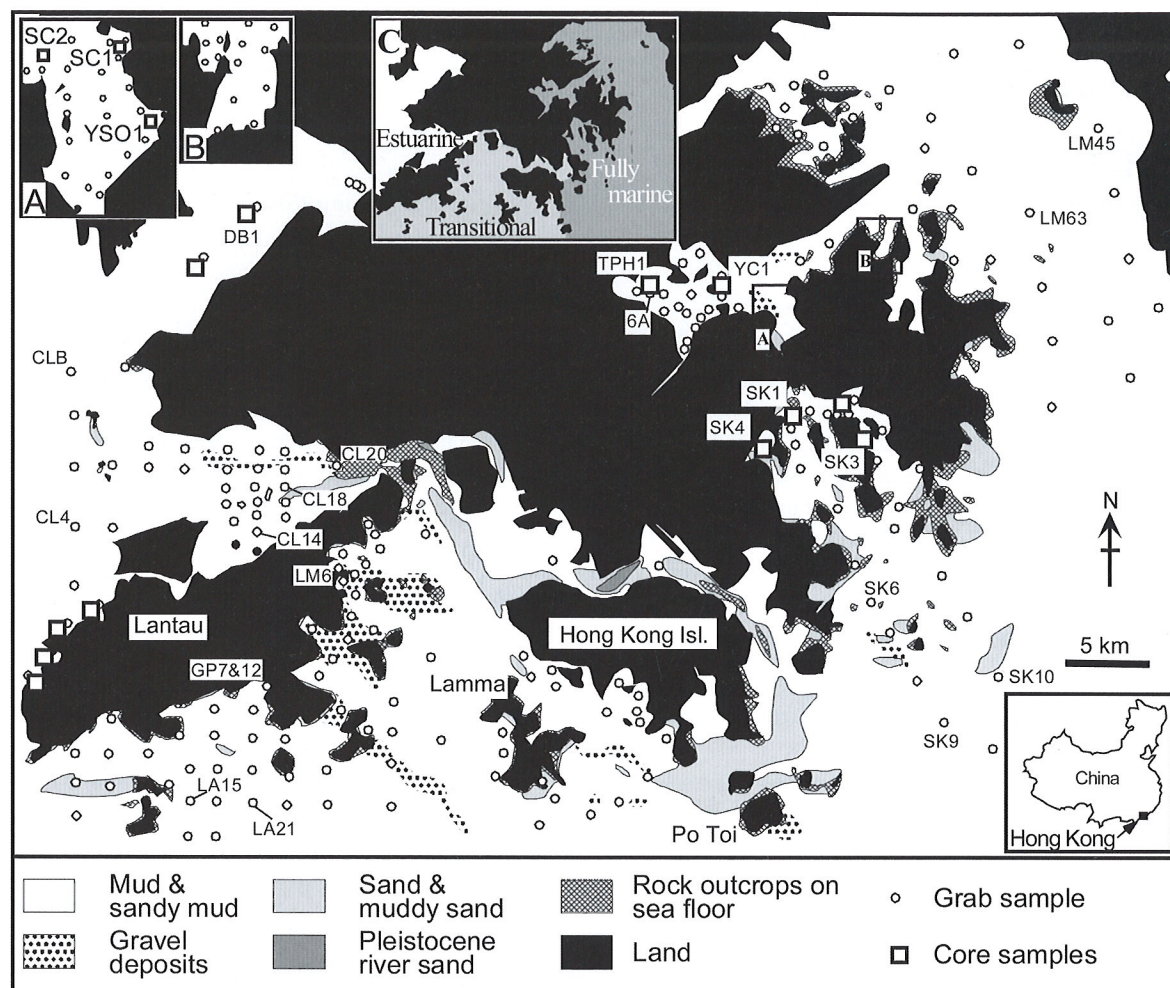


Fig. 1 Seafloor geology (after Fyfe *et al.*, 2000) and surficial sediment sample locations. Inset "C" shows major marine environmental settings (after Morton and Wu, 1974).

of suspended sediment and 30 million tons of dissolved load per year (Shaw and Fyfe, 1992), with peak flow occurring in the rainy summer months. At this time a fresh water wedge extends further seawards, influencing more extensive areas in the transition zone to the southeast of Lantau Island (Fig. 1).

Hong Kong experiences a semi-diurnal (spring tides) to diurnal (neap tides) microtidal (<2 m) regime. Tidal current velocities range between 0.1-2.2 m s<sup>-1</sup> (Fyfe *et al.*, 2000) and are important in controlling seabed morphology. For example, higher velocities (0.5-0.8 m s<sup>-1</sup>) tend to be associated with tidal channels. In some cases residual tidal flow and sedimentation is insignificant (Chalmers, 1984). Many tidal channels appear to represent ancient river systems (Owen *et al.*, 1998), with tidal flow preventing modern deposition of fines in the channels and exposing ancient river sands (Fig. 1).

Oceanic currents are generally insignificant in inshore areas where tidal controls dominate, but

gradually become more important to the south of Lamma Island (Fig. 1). In the latter, area ebb tides flow to the west in winter, and during the summer reverse direction to the east (Fyfe *et al.*, 2000). The winter situation reflects the influence of the southwest-moving, cold-water, Taiwan current and the warmer Kuro Shio current. In summer, the oceanic offshore currents reverse and Hong Kong is influenced by northeast moving water of the Hainan current (Morton and Wu, 1974).

The resulting geology of the offshore areas are complex (Fig. 1), with linear sand belts reflecting old channel alignments and sheet sands providing evidence of transgressive deposition along foreshores and beaches. Lag gravels indicate high tidal current velocities locally, with pelagic mud blanketing extensive low energy settings. This paper focuses on spatial variability within the mud deposits. These are often considered to be uniform in their sedimentological characteristics, but detailed studies show subtle variations that reflect their overall environmental setting.

## Methods

Surficial sediments were collected for sedimentological analyses from 225 sampling stations between 1999 and 2001 (Fig. 1). These were comprised of 197 grab samples and 28 short (<20cm) gravity cores. Of these, 175 were recovered between May 2000 and November 2001 specifically with the aim of developing a data base on organic matter content in the offshore sediments. In addition, 15 Livingstone Piston cores (94.5 cm to 4 m long) were recovered from shallow marine areas (4–10 m deep) off selected drainage basins. Locations of the surficial samples and piston cores are given in Fig. 1.

Particle size analysis was carried out on all samples using a laser particle sizer. Samples were studied both before and after removal of carbonates with HCl. Routine bulk analyses were carried out on the sediments to determine sediment pH, sediment conductivity, moisture content, and the Mass Loss on Ignition (MLOI) of dry sediment.

Sediment pH was determined from sediment (10 g) washed in distilled water (25 ml). Resulting values consistently lay within the range 6.4–8.2, with most values falling between 7.0–7.6. Conductivity data were obtained by washing 50 g of sediment in 50 ml of distilled water. After 24 hours, conductivity readings were taken from the aqueous filtrate. Conductivity of the sediments ranged between 0.1 and 89.4 ms/cm. Low values occurred near fluvial inputs, with most sample values ranging between 20 and 50 ms/cm. Moisture content was determined after weighing and drying sediments at 80°C for 24 hours. Carbonate was determined from dried samples, following the addition of 1M HCl, washing and subsequent re-drying. Decarbonated dry samples were then heated to 600°C in order to determine MLOI.

Carbon and total nitrogen were determined using a PE2400 Series II CHN elemental analyser linked to a microbalance system. Carbonate was first removed with HCl, followed by sample drying at 80°C. The bulk sample (about 2 mg) was then placed in tin boats and weighed accurately. Calibration of the CHN analyser was carried out using Cystine (29.99 wt.% C) with control checks being carried out after every 15th sample.

Diatom data was obtained from studies of smear slides using styraX diatom mountant. Counts were carried out at 400x magnification after initial identifications at 1000x.

Subsamples were collected from piston and gravity cores for the determination of  $^{210}\text{Pb}$  and  $^{137}\text{Cs}$  profiles. Untreated samples were sent to the Nanjing Institute of Technology, China for analysis.

## Seabed deposition and particle size variability

Mud dominates in the offshore areas of Hong Kong. However, quartzo-feldspathic sand and muddy sand is present locally, having formed in sublittoral environments, and deeper-water marine sand banks and sand sheets (Shaw, 1988). Pleistocene river sand crops out along linear tidal channels that mark palaeoriver alignments and zones of relatively high current velocities (Shaw, 1988). The mud deposits are generally dominated by quartzo-feldspathic silt and sandy silt, with a uniform clay content of 10–30% (Fyfe *et al.*, 2000). Other common components include shell carbonate, biogenic silica (diatoms, sponge spicules and radiolaria) and organic matter (locally contributing to pyrite formation).

Clay- and silt-sized particles (mostly <50 microns) account for >90% of the shell-free sediment (Fig. 2A). Particle size distributions for sediments, after removal of carbonate, vary in modality (Fig. 2B). In all samples there is a dominant peak between 19–25 microns. Secondary peaks often occur at 4–5 microns and less frequently at about 60–110 microns (Fig. 2B). Unimodal distributions tend to be more common in western areas, particularly north of Lantau Island (>70% of samples). Bimodal distributions are most common in Mirs Bay (eastern Hong Kong), where 7% of sediment samples are unimodal and 83% are bimodal. In the latter case, the secondary modal peak varies, occurring at 4–5 microns (59% of samples) or 60–110 microns (24%). In many cases samples are trimodal. Central marine areas show particle-size characteristics for carbonate-free mud that are transitional between those described above. In the Lamma area, for example, (Fig. 1) 11% of seabed samples are unimodal. Further west and to the south of Lantau Island, unimodal patterns account for 55% of the deposits.

Regional variability in particle size characteristics can also be seen in plots of mean grain size against standard deviation (Fig. 2C). Sediments in eastern Hong Kong tend to be slightly finer grained and less well-sorted than those present in western locations. Deposits found on the Central Hong Kong seabed show intermediate characteristics.

The grain size distribution pattern reflects various mixtures of biogenic and siliclastic materials. Intact diatoms fall mainly into the size range of 5–30 microns, with chains of colonial species, such as *Skeletonema costatum* and *Paralia sulcata*, reaching up to about 100 microns in length (Plate 1G and H). Fragments contribute to the smallest size categories. Sponge spicules (Plate 1C, K, L)



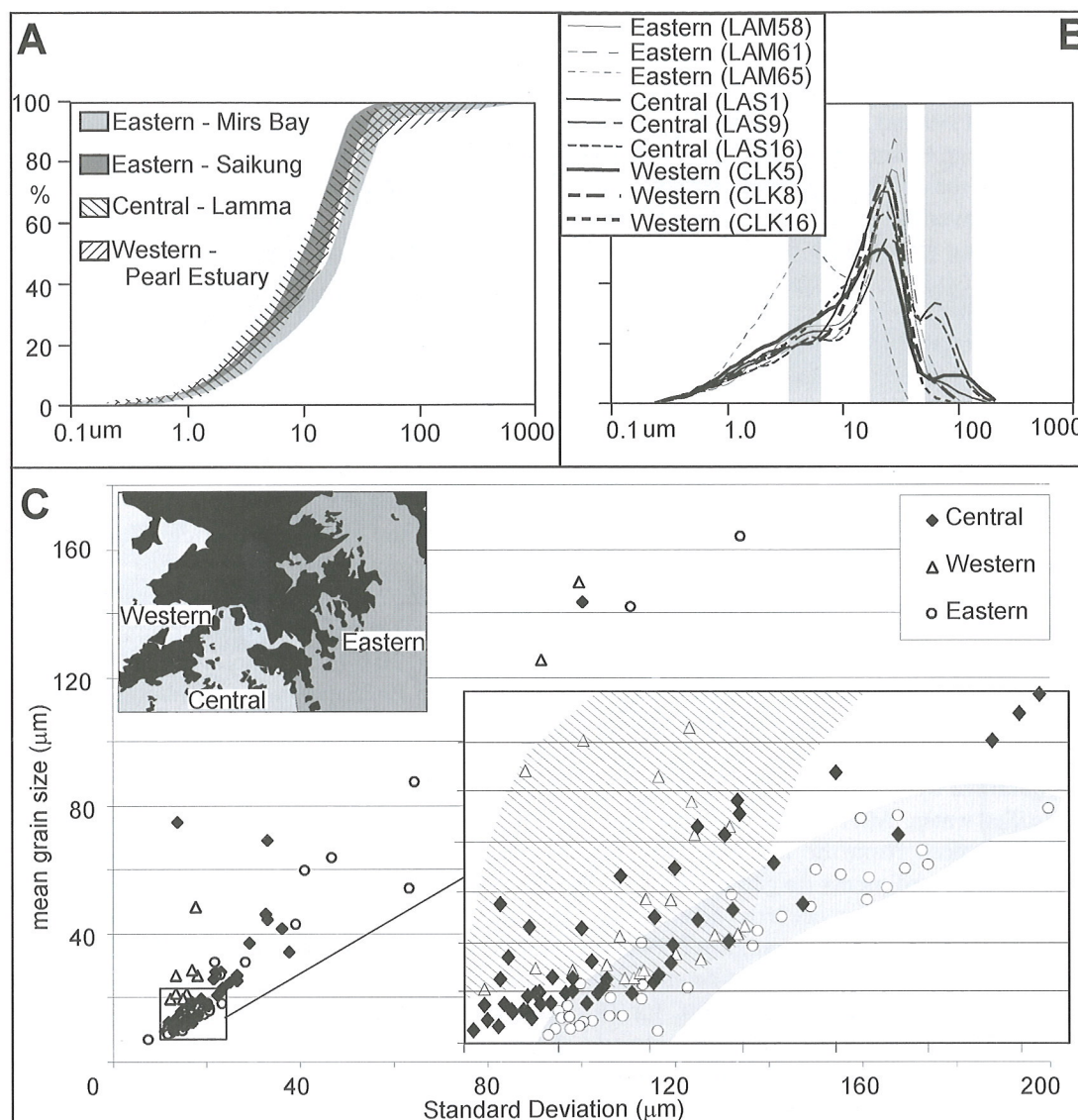


Fig. 2 Particle size characteristics of offshore marine muds in Hong Kong. A: Regional variation in cumulative grain size for mud samples (carbonate removed). B: Detailed grain size characteristics for selected samples. C: Scatterplot data showing contrasts between marine muds found in the Western and Eastern Sectors (see inset), with transitional characteristics for the Central Sector.

typically reach a length of about 100 microns, but often break into 3 or 4 cylindrical fragments with lengths of about 20-40 microns. Quartz and feldspar clasts are typically < 30 microns in length. Siliclastics dominate to a greater extent in western areas that are influenced by suspended sediments of the Pearl River Estuary. Eastern and southern parts of Hong Kong tend to show more abundant diatom frustules in the sediments.

### Sedimentation rates

Fyfe et al. (2000) point out that sedimentation rates in Hong Kong are generally low, with net deposition being higher in the Pearl Estuary, and

particularly near Macau. Much of the eastern part of Hong Kong receives comparatively small fluvial inputs. Fyfe et al. (2000) also note that tidal flushing keeps areas such as Victoria Harbour clear of net deposition.

Table 1 presents sedimentation rate data, based on  $^{210}\text{Pb}$  methods. No clear record was obtained for the waters around Lantau Island, possibly due to bioturbation and/or high sedimentation rates diluting the  $^{210}\text{Pb}$  signals. Sedimentation rates off Sai Kung are low and decline with distance from the coast. In Tolo Harbour, the rates are somewhat higher, ranging between 0.25 and 0.51 cm/a. In Deep Bay a single comparatively low rate of 0.27 was obtained.



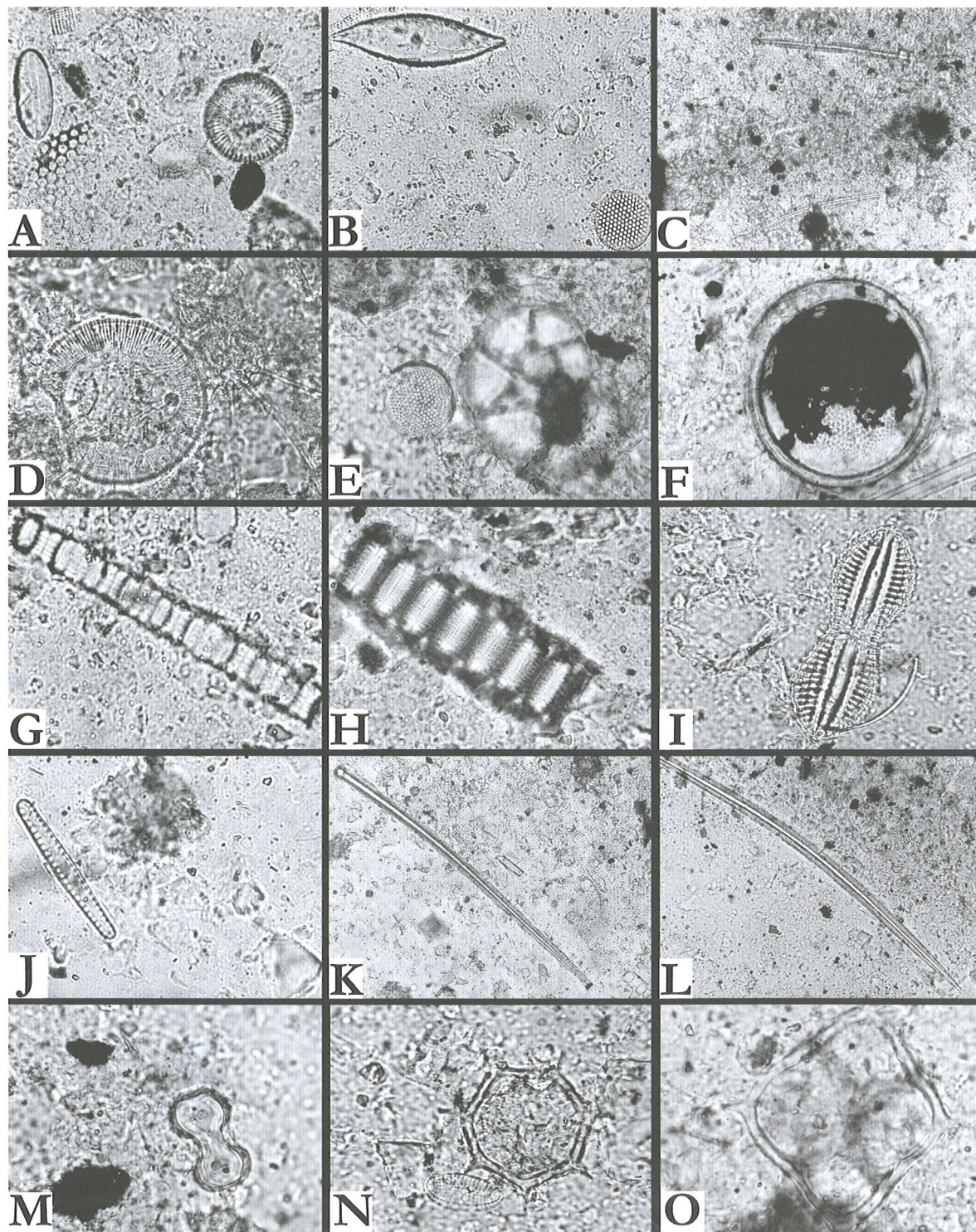


Plate 1 Smear slides of Hong Kong marine muds. A: Typical mixed assemblage of fragmentary and intact diatoms together with clastic materials (400x); B: Intact *Coscinodiscus* and *Gyrosigma* diatoms with silt and clay particles (400x); C: Sponge spicules (200x); D: Well-preserved *Cyclotella* and *Chaetoceras* diatoms in silt/clay matrix (1000x); E: Mixed foraminifera, diatoms (prominent *Coscinodiscus*), and silt; F: Pyrite infilling diatom frustule (1000x); G: Well preserved *Skeletonema costatum* (1000x); H: Well preserved *Paralia sulcata*; *Diploneis* diatom starting to fragment releasing connective girdle band (curved rod to right)(1000x); *Thalassionema nitzschioides* together with silt and clay; K: Sponge spicule (400x); L: Sponge spicule (400x); M: phytolith (1000x); N: Silicoflagellate (1000x); O: Silicoflagellate (1000x).



CORE	Pb210 (cm/a)
<b>Offshore Sai Kung</b>	
SK9	0.17
SK6	0.22
SKP1	0.25
SKP4	0.36
<b>Chek Lap Kok</b>	
CLK18	**
CLKB	**
<b>Lantau south</b>	
LANS26	**
LANS31	**
<b>Tolo Harbour</b>	
SC1	0.51
SC2	0.27
6A	0.34
TPH1	0.33
YC1	0.25
YSO1	0.45
<b>Deep Bay</b>	
DB1	0.27

Table 1 - Lead210 sedimentation rates for marine muds in Hong Kong (\*\* indicates bioturbated cores). See Fig. 1 for locations.

The range of 0.17-0.51 cm/a is comparatively high when contrasted against average Holocene deposition rates. Holocene estimates range between 0.12 and 0.25 cm/a, though this was probably subject to considerable variability related to stage of postglacial flooding (Owen *et al.*; 1998, Fyfe *et al.*, 2000).

### Biogenic silica

Diatoms dominate the biogenic silica component (>85%) of the marine sediments, with at least 106 taxa occurring in the surficial mud (Table 1). Silica is also derived from sponge spicules (Plate 1C, K, L) in very variable quantities (0-95% of the biogenic component) and to a lesser extent from silicoflagellates (<1%) (Plate 1N, O). Glenwright and Dickman (1995) report high diatom species diversities in seabed mud from south eastern Hong Kong, with a decreasing diversity along a transect line from the Nine Pin Islands to Kowloon Bay. Surficial sediment samples from their stations 77 and 81 contain 89 and 84 diatom taxa respectively. In this study, mud at a nearby site (S1 in Fig. 3) contains only 65 diatom species, considerably fewer than the number observed by Glenwright and Dickman. This may be due to the number of counts (not reported) being higher than in their study. If so, the data for the number of diatom species per sample

given in this paper must be treated as a comparative minimum estimate.

Data on the number of species (per diatom count of 250), and summaries of floral composition, are given in Fig. 3. Very shallow water, littoral and shoreline sediments (<5 m) were not sampled, except in the Mai Po area (north west Hong Kong). The dominant diatoms (Fig. 3) in the surficial sediment samples include *Cyclotella striata*, *C. striata* var. *baltica*, *C. comta*, *Paralia sulcata*, *Coscinodiscus lineatus*, *C. radiatus*, *Thalassionema nitzschioides*, *Synedra tabulata* and *Skeletonema costatum*.

There is a strong tendency for *C. striata*, *C. striata* var. *baltica* and *C. comta* to dominate in the west of Hong Kong. *Skeletonema costatum*, often a pollution indicator, is locally common there and to the south of Lantau Island. Floras from other parts of Hong Kong are more variable, but tend to contain abundant *Paralia sulcata* together with common and varied *Coscinodiscus* taxa. Occasional broken (& unidentified) *Chaetoceras* spp. also occur.

Pennate diatoms are relatively uncommon in the offshore sediments that dominate the samples. The most frequent species being *Thalassionema nitzschioides* and *Synedra tabulata*, with much less common *Nitzschia*, *Navicula*, *Fragilaria*, *Grammatophora*, *Gyrosigma*, *Pleurosigma*, *Triceratium* and *Diploneis*. Other genera are present but are comparatively rare in the deposits studied (Table 1).

The diversity of taxa is greatest in southern and southeastern Hong Kong, where diatom counts typically recorded 50-65 species. The lowest numbers of taxa occurs in western estuarine areas, with some samples containing only *C. striata* and its variety *baltica*. The Central marine sector shows transitional characteristics with moderate diatom diversity.

In contrast, late Quaternary deposits contain dramatically fewer diatoms. The Holocene Hang Hau Formation contains at least 74 diatom species (Owen *et al.*, 1998). The Sham Wat Formation (as defined in western Hong Kong) is of controversial age. Owen *et al.* (1998) suggest that it belongs to the latest Pleistocene, whereas Fyfe and James (1995) infer a date of about 120,000 yrs. B.P. The diatom flora from this unit is sparse and of low diversity with only 19 taxa being observed, and with a heavy dominance by *C. striata*.

The Waglan Formation is the oldest unit containing diatoms that has been sampled in this study. TL and OSL dates range from about 80,000 to 95,000 yrs. B.P. (Owen *et al.*, 1998). Only four samples were examined from this unit, which contains very few diatoms consisting of 4 taxa: *C. striata* and *C. comta*, with rare *Coscinodiscus lineatus* and *C. temperei*. This progressive loss of

Centric diatoms	SURFICIAL SEDIMENT	HANG HAU F.	SHAM WAT F.	WAGLAN F.
Actinocyclus ehrenbergii	*	*	-	-
Actinocyclus ehrenbergii v. crassa	-	*	-	-
Actinocyclus ehrenbergii v. ralfsi	-	*	-	-
Actinocyclus ehrenbergii v. tenella	*	-	-	-
Actinocyclus octonarius v. crassus	*	*	-	-
Actinoptychus undulatus	*	*	-	-
Actinoptychus pericavitus	*	-	-	-
Arachnoidiscus ornatus	*	*	-	-
Biddulphia obtusa	*	*	-	-
Biddulphia laevis	*	*	*	-
Chaetoceras affinis	*	*	-	-
Chaetoceras spp.	*F	*F	-	-
Coscinodiscus asteromphalus	*	*	-	-
Coscinodiscus agapetos	*	-	-	-
Coscinodiscus bathyomphalus v. hispidus	*	-	-	-
Coscinodiscus bipartius	*	-	-	-
Coscinodiscus blandus	*	*	*	-
Coscinodiscus centralis	**	**	*	-
Coscinodiscus crenulatus	*	*	-	-
Coscinodiscus decrescens	*	-	-	-
Coscinodiscus excentricus	*	*	-	-
Coscinodiscus kutzingii	*	*	*	-
Coscinodiscus lineatus	**	**	-	*
Coscinodiscus marginatus	*	*	*	-
Coscinodiscus marginato-lineatus	**	*	-	-
Coscinodiscus minor	*	*	*	-
Coscinodiscus nitidus	*	-	-	-
Coscinodiscus radiatus	**	*	*	-
Coscinodiscus rothii	*	-	-	-
Coscinodiscus subconcaus	*	-	-	-
Coscinodiscus subtilis	*	-	-	-
Coscinodiscus temperei	*	*	-	*
Coscinodiscus wittianus	**	*	-	-
Cyclotella comta	*	**	*	*
Cyclotella comta v. oligactus	*	-	-	-
Cyclotella meneghiniana	*	*	-	-
Cyclotella striata	***	***	**	*
Cyclotella striata v. baltica	***	**	*	-
Cyclotella stylorum	**	*	*	-
Cymbella affinis	*	*	-	-
Hyalodiscus radiatus	*	*	-	-
Melosira islandica	*	-	-	-
Melosira moniliformis	*	-	-	-
Melosira nummuloides	*	*	-	-
Paralia sulcata	***	***	**	-
Podosira stelliger	*	*	-	-
Skeletonema costatum	**	*	-	-
Skeletonema subsalsum	*	-	-	-
Skeletonema tropicum	*	-	-	-
Stephanopyxis grunowii	*	*	*	-
Thalassiosira excentrica	*	*	-	-

Table 2 - Centric diatom taxa in offshore sediments, Hong Kong. R - rare; F - fragments only; \* - present; \*\* - common; \*\*\* - abundant.



Pennate diatoms	SURFICIAL SEDIMENT	HANG HAU F.	SHAM WAT F.	WAGLAN F.
Achnanthes brevipes v. angustata	*	-	-	-
Achnanthes brevipes v. intermedia	*	*R	-	-
Amphora crassa	*	*	-	-
Amphora coffeaeformis	*	-	-	-
Amphora costata	*	-	-	-
Caloneis elongata	*	*F	-	-
Campyloneis grevillei	*	*	-	-
Cocconeis scutellum	*	*	-	-
Cocconeis scutellum v. varians	*	-	-	-
Cymbella affinis	*	*	-	-
Diploneis bombus	**	*	*	-
Diploneis smithii	*	*	*	-
Diploneis splendida	*	*	-	-
Eunotia sp.	*R	*R	-	-
Fragilaria oceanica	*	*	-	-
Grammatophora marina	*	*	*	-
Grammatophora undulatus	*	*	-	-
Gyrosigma sp.	*	-	-	-
Mastogloia decussata	*	*	-	-
Navicula directa	*	-	-	-
Navicula directa v. javanica	*	-	-	-
Navicula hennedyi	*	*	-	-
Navicula lyra	-	*	-	-
Navicula marina	*	*	-	-
Navicula raena	*	-	-	-
Nitzschia cocconeiformis	*	*	*	-
Nitzschia constricta	*	-	-	-
Nitzschia frustulum	*	-	-	-
Nitzschia granulata	*	*	*	-
Nitzschia lanceolata	*	*	-	-
Nitzschia lanceolata v. minor	*	-	-	-
Nitzschia linearis	*	-	-	-
Nitzschia panduriformis	*	*	-	-
Nitzschia punctata	*	*	*	-
Nitzschia sigma	*	-	-	-
Pinnularia viridis	*	*	-	-
Plagiogramma wallichianum	*	*	-	-
Pleurosigma aestuarii	*	*F	-	-
Pleurosigma normanii	*	-	-	-
Pseudostaurosira brevistriata	**	*	-	-
Rhaphoneis rhomboides	*	*	-	-
Rhizolsolenia sp.	*F	*F	-	-
Rhopalodia musculus	*	*	-	-
Rhopalodia sp.	*F	-	-	-
Surirella fastuosa	*	*	-	-
Surirella fastuosa var. recens	*	*	-	-
Synedra acus	*	*	-	-
Synedra tabulata	**	**	-	-
Synedra tabulata v. obtusa	*	*	-	-
Synedra ulna	*	*	-	-
Thalassionema nitzschioides	**	**	-	-
Trachyneis antillarum	*	-	-	-
Trachyneis debyi	*	-	-	-
Triceratium favus	*	*	-	-
Triceratium perpendiculare	*	*	-	-

Table 3 - Pennate diatom taxa in offshore sediments, Hong Kong. R - rare; F - fragments only; \* - present; \*\* - common; \*\*\* - abundant



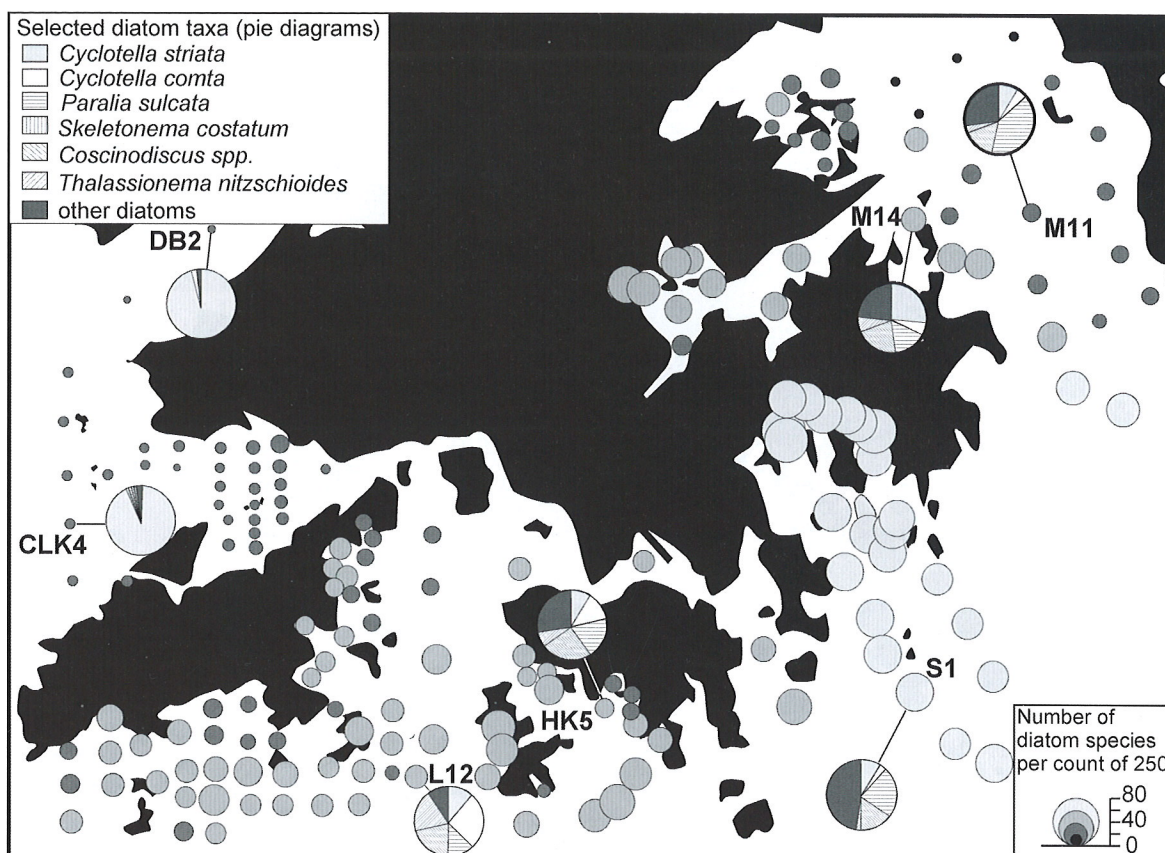


Fig. 3 Spatial variation in diatom species in offshore surficial muds

### Carbonate sedimentation

diatoms with depth was reported in some detail by Yim and Li (2000) and suggests dissolution is an important process in the marine mud of Hong Kong.

Potential sources of carbonate are varied, but include bivalves, gastropods, coral and foraminifera (Plate 1E; Table 3). Macrofossils occur in several states of preservation, including finely comminuted, disarticulated

<i>Foraminifera</i> / Location	CL20	CL14	CL5	LA15	LA21	LM45	LM6	LM63	GP7	GP12	SK3	SK10
<b>I. Textulariina</b>												
Textulariina sp.	1	0	0	5	0	0	0	0	0	0	0	7
Ammobaculites sp. nov.	0	0	6	2	0	0	0	2	0	0	0	1
Haplophragmoides												
shenzhensis sp. nov.	0	0	1	1	0	0	0	2	0	0	0	4
<b>Total no. of Textulariina</b>	<b>1</b>	<b>0</b>	<b>7</b>	<b>8</b>	<b>0</b>	<b>0</b>	<b>0</b>	<b>4</b>	<b>0</b>	<b>0</b>	<b>0</b>	<b>12</b>
<b>II. Miliolina</b>												
Quinqueloculina sp.	19	2	23	29	12	26	0	4	23	3	26	9
Spiroloculina sp.	5	0	3	6	11	0	0	0	0	0	0	0
<b>Total no. of Miliolina</b>	<b>24</b>	<b>2</b>	<b>26</b>	<b>35</b>	<b>23</b>	<b>26</b>	<b>0</b>	<b>4</b>	<b>23</b>	<b>3</b>	<b>26</b>	<b>9</b>
<b>III. Rotaliina</b>												
Ammonia sp.	24	39	111	74	32	95	114	290	46	20	125	33
Elphidium sp.	34	93	87	47	21	99	67	17	210	116	113	37
Flovilus sp.	0	0	0	25	7	8	0	12	0	0	13	9
Rosalina sp.	1	0	0	0	0	0	0	0	0	0	0	3
Brizalina sp.	0	0	0	0	0	24	0	14	0	0	3	0
<b>Total no. of Rotaliina</b>	<b>59</b>	<b>132</b>	<b>198</b>	<b>146</b>	<b>60</b>	<b>226</b>	<b>181</b>	<b>333</b>	<b>256</b>	<b>136</b>	<b>254</b>	<b>82</b>
<b>Total number</b>	<b>84</b>	<b>134</b>	<b>231</b>	<b>189</b>	<b>83</b>	<b>252</b>	<b>181</b>	<b>341</b>	<b>279</b>	<b>139</b>	<b>280</b>	<b>103</b>
Total wt of sediment sample (g)	1	1	1	0.5	1	0.2	0.5	0.1	1	1	0.2	1
<b>No of Forams/g</b>	<b>84</b>	<b>134</b>	<b>231</b>	<b>378</b>	<b>83</b>	<b>1260</b>	<b>362</b>	<b>3410</b>	<b>279</b>	<b>139</b>	<b>1400</b>	<b>103</b>

Table 3 Variability in Foraminifera in offshore marine mud in Hong Kong. See Fig 1 for sample locations.

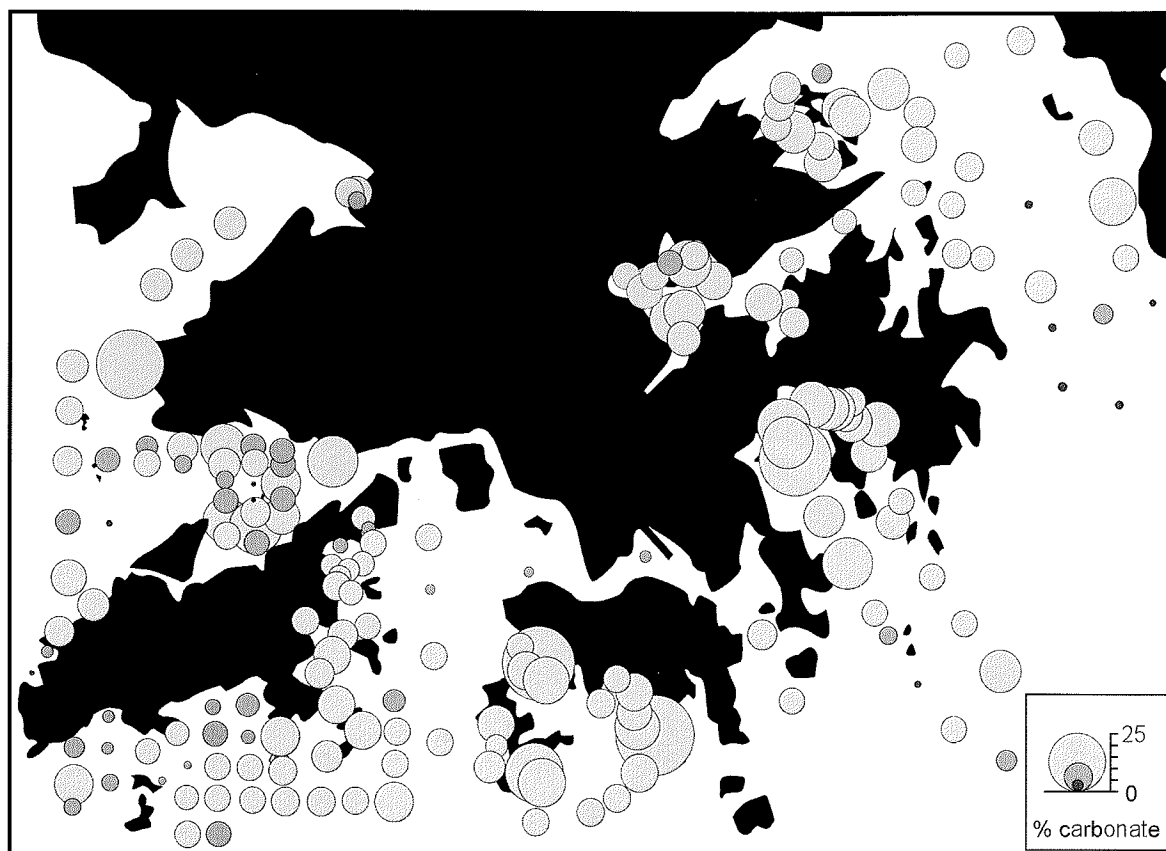


Fig. 4 Spatial variation in carbonate in offshore surficial muds

and intact. Carbonate concentrations in the marine sediments of Hong Kong are shown in Fig. 4. The percentage of carbonate is highly variable, even at local scales with most mud samples containing between 2 and 25% carbonate (though pure coquinas also develop locally).

In general, the highest levels of carbonate appear to be correlated with the more oceanic environments that are encountered in eastern and southern Hong Kong. The brackish Pearl River Estuary and southern Lantau area have generally lower carbonate contents, that may reflect either habitat preferences of the main organisms contributing to the carbonate deposits, and/or dilution by sediment.

### Organic matter and Organic carbon

Carbon occurs in a variety of forms in the marine sediments in Hong Kong. These include biologically-derived particulate organic matter, inorganic carbonate (noted above) and bicarbonate, and gaseous forms such as  $\text{CO}_2$  and methane. These carbon accumulations develop in response to a variety of factors, such as the local sedimentation rate, the nature and character of organic source

types and their flux rates, the preservation potential of the organic materials during transport and burial, and the post-depositional processes involved in diagenesis.

Organic carbon (OC) in Hong Kong marine mud shows a good positive correlation with Mass Loss on Ignition (MLOI) (inset, Fig. 5). In general, MLOI measures organic matter (OM), which is comprised of O, H, N, P and other elements in addition to C. OM exceeds OC values (wt %) by about 8-10 times. MLOI results range between 2 and 32 wt. %, with most samples containing between 5 and 15% (corresponding to OC values of about 0.6 and 1.6%). Organic matter shows two trends in the marine sediments (Fig. 5). In general, OM values are highest in the eastern oceanic settings and lowest in the brackish western sector. Organic matter also tends to be higher in nearshore locations, though it is important to note that intertidal settings were not sampled, except at a small number of locations.

### Discussion

Hong Kong's marine mud is composed of mixtures of siliclastic fragments, carbonate, biogenic



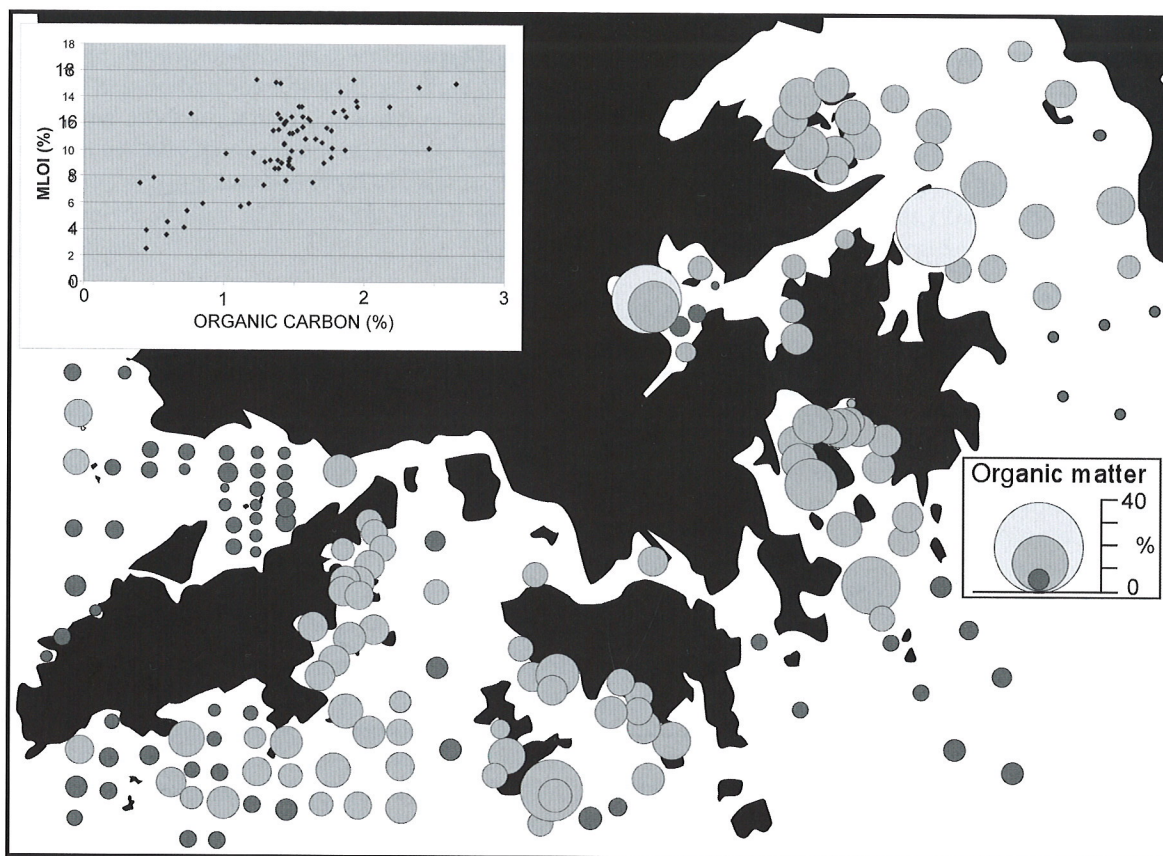


Fig. 5 Spatial variation in organic matter in offshore surficial muds. Inset shows the correlation between organic matter (MLOI) and organic carbon for Hong Kong.

materials, and organic matter (including organic carbon). Minor quantities of authigenic materials such as pyrite are also present. Distinct trends occur across the SAR's territorial waters in terms of these components and in terms of particle sizes and sedimentation rates. In some cases variability is clear and regional (e.g. organic matter, diatom content). In other cases components show significant local as well as regional variability (e.g. carbonate). Variability can be subtle and require detailed analyses to determine (e.g. grain size characteristics). In general, these variations reflect the combined influences of oceanic versus estuarine sedimentation and nearshore versus offshore environments. These determine sediment supply rates for the various components and also the potential for sediment accumulation. Superimposed on these major locational controls are the effects of local tidal currents and tidal regime, wave action (reflecting water depth and aspect of sites), and biological activity.

Biological silica (diatoms, sponge spicules) is a comparatively minor component of the flux to the marine sediments, with the bulk of the material being derived from siliclastics (feldspar, quartz, clay, etc.). Carbonate and siliclastic deposition rates will in turn

determine the degree to which organic carbon/matter is diluted during deposition. Heinrichs and Reeburgh (1987) suggest that sedimentation rate and associated organic material flux, are the primary controls. Ricken (1993) pointed out that organic matter, carbonate and siliclastic materials can be considered end members in a three-component system that reflected variations in sedimentation style. He used carbonate-organic matter cross plots to distinguish three basic types of deposition:

1. *Carbonate deposition.* OM is increased or decreased by variations in carbonate supply rates, with an inverse relationship developing between carbonate and OM (expressed as wt %).

2. *Siliclastic deposition.* Carbonate and organic matter supply rates are constant with siliclastic flux varying. Cross plots of carbonate and OM show a positive correlation.

3. *Organic matter deposition.* Changes in OM flux occur, but are small compared with the larger changes in carbonate and siliclastics. There is only a slight effect on carbonate concentration and OM varies independently of carbonate. A near vertical regression line results on cross plots of carbonate and OM. Figure 6 shows carbonate/OM scatter

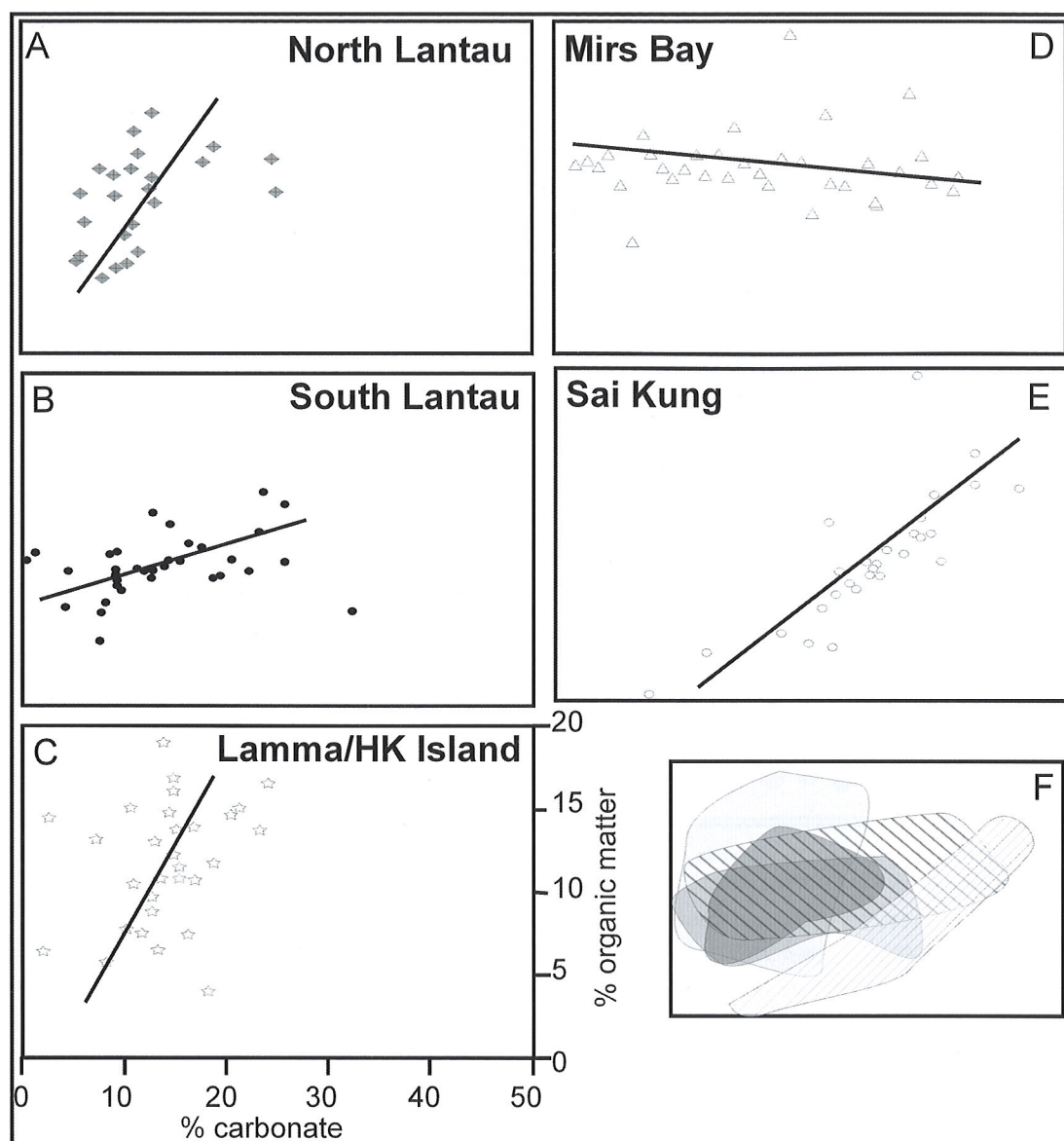


fig. 6 Organic matter-carbonate correlations for selected regions in Hong Kong. A-E show detailed of scatter diagram results. Note the distinct differences between regions, with western areas affected by the Pearl River showing the greatest similarities. F shows a summary diagram with overlapping fields. Shaded areas correspond with A-C, with hatched fields equating to D and E.

plots. Samples from western Hong Kong are characterised by low carbonate contents and positive correlations suggesting siliclastic sedimentation. Samples from Sai Kung also show a positive correlation, but with higher carbonate contents developing. The sediments of Mirs Bay show a slight negative correlation indicating that carbonate style deposition is of some importance in this area.

Organic matter content is generally dependent on carbonate content (Ricken, 1993), with positive correlations in siliclastic-dominated

deposition or negative correlations in carbonate-dominated deposition. The importance of siliclastic sedimentation in Hong Kong reflects its inner shelf location and the influence of the Pearl River.

Other factors that play a role in these relationships include the organic source flux, preservation during burial and post-depositional diagenesis.

In summary, The offshore marine mud show subtle, but distinct variations in their sedimentological characteristics. Variability can be

seen in particle size parameters, organic matter, carbonate, biogenic silica, and sedimentation rates.

These variations reflect large scale changes in marine environment (nearshore vs. offshore; brackish vs. fully marine; high vs. low wave energy) and local setting (within tidal channels, broad bathymetric plains, aspect with regard to wave direction etc.).

## Acknowledgements

The author would like to thank Ms. Alison Lee for laboratory work and identification of Foraminifera. Dr. R. Shaw made useful comments on this manuscript. The work was funded by a H.K. Baptist University research grant (FRG/99-00/II-02) and by an RGC grant (HKBU 2016/00P).

## References

- Chalmers, M.L. (1984) Preliminary assessment of sedimentation in Victoria Harbour, Hong Kong. In: W.W.S. Yim (Ed.) *Geology of Surficial Deposits in Hong Kong*. Geological Society of Hong Kong Bull. No. 1, 117-129.
- Fyfe, J.A. and James, J.W.C. (1995) The offshore Quaternary Sham Wat Formation of Hong Kong. *Hong Kong Geologist*, 1, 30-33.
- Fyfe, J.A., Shaw, R., Campbell, S.D.G., Lai, K.W. and Kirk, P.A. (2000) *The Quaternary Geology of Hong Kong*, Geotechnical Engineering Office, Civil Engineering Department, The Government of the Hong Kong SAR.
- Glenwright, T. and Dickman, M. (1995) Diatom assemblages in surficial sediments along a transect between the Nine Pin Island Group and Kowloon Bay, Hong Kong. In: B. Morton (Ed), *The Marine Flora and fauna of Hong Kong and Southern China IV*. Proceedings of the Eighth International Marine Biological Workshop, April 1995. Hong Kong University Press.
- Heinrichs, S.M. and Reeburgh, W.S. (1987) Anaerobic mineralization of marine sediment organic matter: Rates and the role of anaerobic processes in the organic carbon economy. *Geomicrobiol. J.*, 5, 191-237.
- Lam, H. W. (1994) *Marine water quality in Hong Kong for 1993*. Environmental Protection Department, Hong Kong Government, 102 p.
- Morton, B. and Wu, S.S. (1974) The hydrology of the coastal waters of Hong Kong. *Environmental Research*, 10, 319-347.
- Owen, R.B., Neller, R., Shaw, R. and Cheung, P.C.T. (1998) Late Quaternary environmental changes in Hong Kong. *Palaeogeography, Palaeoclimatology, Palaeoecology*, 138, 151-173.
- Parry, S. (2000) The origin and variability of suspended sediment in Hong Kong's marine waters. In: A. Page and S. Reels (Eds.) *The Urban Geology of Hong Kong*. Geological Society of Hong Kong Bulletin No. 6, 123-139.
- Ricken, W. (1993) *Sedimentation as a Three-Component System, Organic Carbon, Carbonate, Noncarbonate*. Lecture Notes in Earth Sciences, 51, Springer Verlag, 211p.
- Shaw, R. (1988) The nature and occurrence of sand deposits in Hong Kong waters. In: P.G.D. Whiteside, and N. Wragge-Morley (Eds.) *Marine sand and gravel resources of Hong Kong*. Proceedings of the Seminar on Marine Sources of Sand. Geological Society of Hong Kong, pp. 33-43.
- Shaw, R. and Fyfe, J.A. (1992) *The influence of the Pearl River on the offshore geology of the Macao-Hong Kong area*. Proceedings of the International Conference on the Pearl River Estuary in the surrounding area of Macao, Macao, October, 1992, Laboratorio de Engenharia Civil de Macao, Macao, pp. 247-255.
- Yim, Y.Y.S. and Li, J. (2000) Diatom preservation in an inner continental shelf borehole from the South China Sea. *Journal Asian Earth Sciences*, 18, 471-488.



## Preliminary conceptual study on impact of land reclamation on groundwater flow and contaminant migration in Penny's Bay

J.J. Jiao

*Department of Earth Sciences, University of Hong Kong, Hong Kong*

### Abstract

A large-scale land reclamation project is now being carried out at Penny's Bay, Lantau Island, Hong Kong. The completed reclamation will provide 2.8 km<sup>2</sup> of land for the construction of the new Hong Kong Disneyland and other essential infrastructure developments. The impact of this project on various aspects, such as ecology and environment has been widely discussed. This paper studies change in the groundwater system around the bay area in response to the land reclamation. This paper also predicts the possible flow pathway of the contaminated groundwater due to the Cheoy Lee Shipyard, which was located on the north and eastern shores of Penny's Bay and had operated for almost 40 years. Findings observed on basis of this preliminary study include: 1) After reclamation, the total groundwater head in the entire model area increased, and the slopes immediately behind the original coast of the Bay have the most significant buildup in total head. 2) Seepage along the coastlines beyond Penny's Bay will increase in response to the reclamation, with Yam O Wan seepage increased being especially significant. 3) If contaminated soil near the Cheoy Lee Shipyard is not removed, the contaminated groundwater will not spread within Penny's Bay, but will migrate northeast toward Yam O Wan. FEMWATER, a three-dimensional finite element ground water model, is used in this study. It should be noted that this paper is entirely based on desk computer simulation and all the basic data such as aquifer properties and the infiltration coefficient are assumed values. The overall qualitative conclusions of the study are believed to be reasonable, but quantitative values of the computer output such as groundwater head or contaminant travel time may be very uncertain due to lack of actual data and field hydrogeological study from this reclamation site.

### 摘要

目前大嶼山的竹篙灣正進行著大規模的填海。其目的是為香港的迪士尼樂園及其配套設施提供約 2.8km<sup>2</sup> 的土地。本文研究了填海對竹篙灣一帶地下水流動系統的改變。本文也對因財利船廠而污染的地下水在填海之后的可能遷移方向進行了初步預測。本文的研究得出了如下幾點初步結論：1) 填海之后竹篙灣一帶的地下水位有明顯增高，靠近原竹篙灣海岸線斜坡內地下水位升高最為顯著。2) 與竹篙灣相對的海岸線地下水向海排泄量增加，其中陰澳灣一帶排泄量增加尤為明顯。3) 如果財利船廠附近的污染物不加以清除，其污染的地下水將逐漸漫延開來並最終流向陰澳灣。應該指出，本文的研究主要基於假設的水文地質參數，因此，總體的定性的結論是可信的，但定量的計算結果如地下水位及污染物遷移的時間可能不一定可靠。若要得出更為可靠的結論，需要大量的野外地質水文地質資料及更詳細的數值模擬研究。

### Background

In November 1999, the HKSAR Government announced that agreement had been reached with the Walt Disney Company to build a Disney theme park in Hong Kong. Penny's Bay, Lantau Island,

was selected as the best site for constructing such a park. The topography of Penny's Bay is shown in Fig. 1. This project involves several major works elements, including the reclamation of about 2.8 km<sup>2</sup>

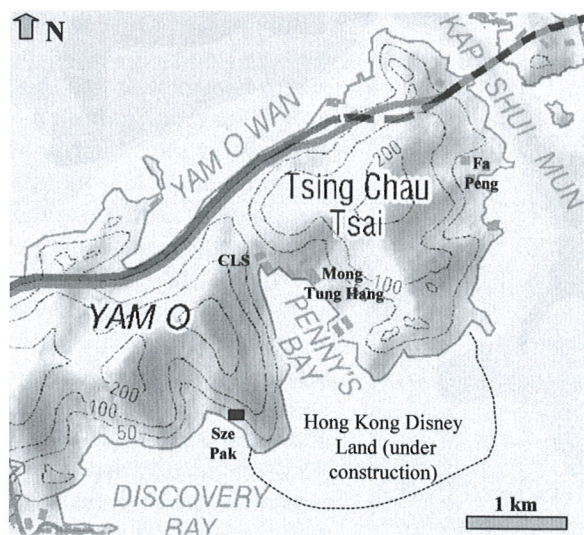


Fig. 1 Topography of Penny's Bay (modified from free map downloaded from [http://www.info.gov.hk/landsd/mapping/mp/html/index\\_fnd.htm](http://www.info.gov.hk/landsd/mapping/mp/html/index_fnd.htm))

of land in Penny's Bay. The project started in May 2000 and the entire works are expected to complete by the end of 2008.

The reclamation methods and fill materials vary over the site. Marine mud in the seawall area will be dredged. The mud in other areas will be largely left in place. Over 70 million m<sup>3</sup> of fill material (including surcharging) will be placed in the reclamation site. The fill materials vary and include marine sand from offshore sites, river sand from Mainland China, decomposed igneous soil, construction waste, and public fill, which would otherwise be disposed of at strategic landfills or fill banks. The elevation of the final ground surface after reclamation will be about 11 mPD.

The bedrock around Penny's Bay is largely feldsparphyric rhyolite. The coastal area near Yam O Wan consists of tuff. The stratigraphy of the Quaternary deposits at the site is primarily a two-fold succession of soft mud of the Hang Hau Formation overlying a complex mixture of firm to stiff silty clay with some sand and silt, which forms the Chek Lap Kok Formation.

A former ship-building site called the Cheoy Lee Shipyard (CLS) was located on the north and eastern shores of Penny's Bay with an area of about 0.19 km<sup>2</sup>. It commenced operation in 1964 and was used for boat manufacture, repair and maintenance. The shipyard was decommissioned in 2001 to make way for roads and other infrastructure linking Penny's Bay to the rest of Hong Kong. In early January 2000, it was reported that the soil on the CLS site had been seriously polluted over the years by oils, heavy metals, dyes and organic solvents brought about by ship-breaking activities and the

disposal and burning of wastes on site. A number of substances require specialized forms of treatment to ensure their eradication from the site. Notable among these is dioxin-contaminated soil, a cancer-causing chemical produced by burning plastic or polyvinyl-chloride (PVC) materials.

The contract for the excavation and demolition of the CLS was awarded in July 2002 with the work commencing in September 2002, involving the removal of around 87,000 m<sup>3</sup> of contaminated soil from the site. However, it is difficult to remove all the contaminated soil entirely. Even if the soil can be removed, the contaminated groundwater around the site may still cause problems.

Large-scale land reclamation may modify the regional groundwater flow system and theoretically such modification usually has adverse engineering and environmental consequences (Jiao, 2000; Jiao *et al.*, 2001). For the Penny's Bay reclamation project, although there are studies on various issues such as marine environment and coastal ecology related to this reclamation project, there seems to be no study directed towards understanding change of the groundwater flow system due to the reclamation.

This paper involves a theoretical desk study of the groundwater flow systems near Penny's Bay before and after the reclamation, and attempts to predict the possible flow pathway for the contaminated groundwater originating from the CLS. The potential engineering problems and environmental effects caused by any change in the groundwater system is also discussed. The investigation in this paper is largely conceptual and by no means comprehensive due to lack of hydrogeological data from the site.

Parameter	Top layer	Bottom layer
Permeability	$10^{-5}$ m/s	$10^{-6}$ m/s
Longitudinal dispersivity	10m	10m
Lateral dispersivity	1 m	1 m
Molecular dispersion coefficient	$0.0001 \text{ m}^2/\text{s}$	$0.0001 \text{ m}^2/\text{s}$

Table 1 Key aquifer hydraulic and transport parameters used in the model

### Assumptions and parameters used in this study

This conceptual numerical study is based on many assumptions. All the coastlines are treated as fixed-head boundaries, with constant head of 1.23 mPD. The west boundary is chosen to be over 3km from Penny's Bay, and is represented by a no-flow boundary. The bottom boundary of the model is selected to be -20 mPD and impermeable. The soil above the impermeable bottom is divided into two layers. The boundary between the lower and upper layers is chosen to be the middle point between the ground elevation and -20 mPD. The geological material in each layer is treated as homogeneous and isotropic. It is assumed that in the upper layer,  $K_x=K_y=10^{-5}$  m/s, and in the lower layer,  $K_x=K_y=10^{-6}$  m/s (Table 1). These values are within the typical permeability range of decomposed granite in Hong Kong (GEO, 1993).

A man-made reclamation area is produced by dumping fill materials. The nature of the soil in a reclamation is usually heterogeneous, and may be even more heterogeneous than soils or sediments developed naturally from geological materials. The permeability in a reclamation is extremely unpredictable and varies with the fill materials used, and the method of placement. On the basis of laboratory testing, the typical range of permeabilities for compacted fill materials of completely decomposed granite and volcanics are  $10^{-6}$  to  $10^{-7}$  and  $10^{-6}$  to  $10^{-8}$  m/s, respectively (GEO, 1993). Marine sand is probably the most permeable material among the commonly used fills.

Shen and Lee (1995) investigation carried out studies of hydraulic fill performance in Hong Kong. They note that the typical permeability of marine sand used in the generalized soil profile in Tseung Kwan O was  $1.0 \times 10^{-4}$  m/s, and that in West Kowloon the permeability was between  $6.0 \times 10^{-5}$  and  $8.0 \times 10^{-5}$  m/s. The permeability value in the field is usually

much lower than that estimated in the laboratory. While the quality and nature of fill at a site can be extremely variable, there is usually a layer of soft marine mud at the seabed beneath reclamation sites. The permeability of the marine mud is usually extremely low, with a range of  $10^{-7}$  to  $10^{-9}$  m/s (Kwong, 1996). This layer of mud is usually troublesome. It gradually becomes less and less permeable as consolidation continues. In this study, the reclaimed site is represented by two layers. The permeability of these two layers is treated as the same as the background soil.

Rainfall is the dominant recharge to the groundwater system. The recharge rate is chosen to be  $1.27 \times 10^{-8}$  m/s, which is about 20% of the average annual rainfall of 2000 mm in Hong Kong. Since this study concerns long-term change of the groundwater flow system, only steady state is simulated. A steady state flow model is run before land reclamation, then another steady state model is run after land reclamation.

FEMWATER, a three-dimensional finite element ground water model (Lin *et al*, 1997), is chosen for this modeling study. This code is run via GMS (Groundwater Modeling System) developed by Brigham Young University under the direction of the U.S. Army Corps of Engineers. Before reclamation, the study area is discretised into 3542 nodes and 5124 elements, after reclamation, the model area is discretised into 4382 nodes and 6618 elements.

### Groundwater system before and after reclamation

Fig. 2 shows the total groundwater head distributions in the groundwater system near Penny's Bay before and after reclamation. Before reclamation, the total groundwater head is high at two topographical centers near Tsing Chau Tsai and Yam O, which are located to the east and west of Penny's Bay. There is a groundwater divide between



Penny's Bay and Yam O Wan.

After reclamation, there is a regional increase in total groundwater head. The groundwater divide originally between Penny's Bay and Yam O Wan has moved to a position within Penny's Bay. The high total head originally located at the hilltop of Tsing Chau Tsai has moved to areas immediately behind Mong Tung Hang, which is on the east coast of Penny's Bay.

As can be seen from Figure 2b, a steep hydraulic gradient, which indicates high seepage, toward the coastal slopes can also be observed near Mong Tung Hang. Table 2 lists the percentage increase of total head in a few selected locations shown in Figure 2b. The slopes (Locations A-C) around the Bay experience a great increase in total head. The total head at Location A has been almost tripled. There is also a significant increase in total head in areas far from Penny's Bay (Location D-F). The head at Location E near Sze Pak has increased by almost 60%.

As can be seen from the 16 m contour near the western model boundary before and after reclamation, the head there has the smallest increase in total head, which indicates that the reclamation has limited impact on areas that are far from the Bay. This also shows that the choice for the location of the western boundary of the model is reasonable.

Fig. 3 shows the groundwater flow directions before and after reclamation. The reclamation has led to a change in the flow pattern

Location	A	B	C	D	E	F
Increase in head	196%	178%	153%	16%	58%	35%

Table 2 Percentage increase of total groundwater head in selective points after reclamation

not only near the Bay, but also to areas beyond it. For example, before reclamation, the coastal area near Sze Pak does not show an obvious groundwater catchment, but after reclamation, there is a well-defined groundwater catchment behind the slopes near Sze Pak. Before reclamation, the coastal area behind Fa Peng indicates an obvious groundwater catchment, but after reclamation, the catchment is much larger with strong convergent flow toward the coastline.

Figure 3b also shows that towards the centerline of Penny's Bay, there is a strong groundwater convergent flow (see the shadow strip inside the Bay). It is expected that the groundwater level may be reduced if a zone of very permeable fill materials is placed along this centerline. This

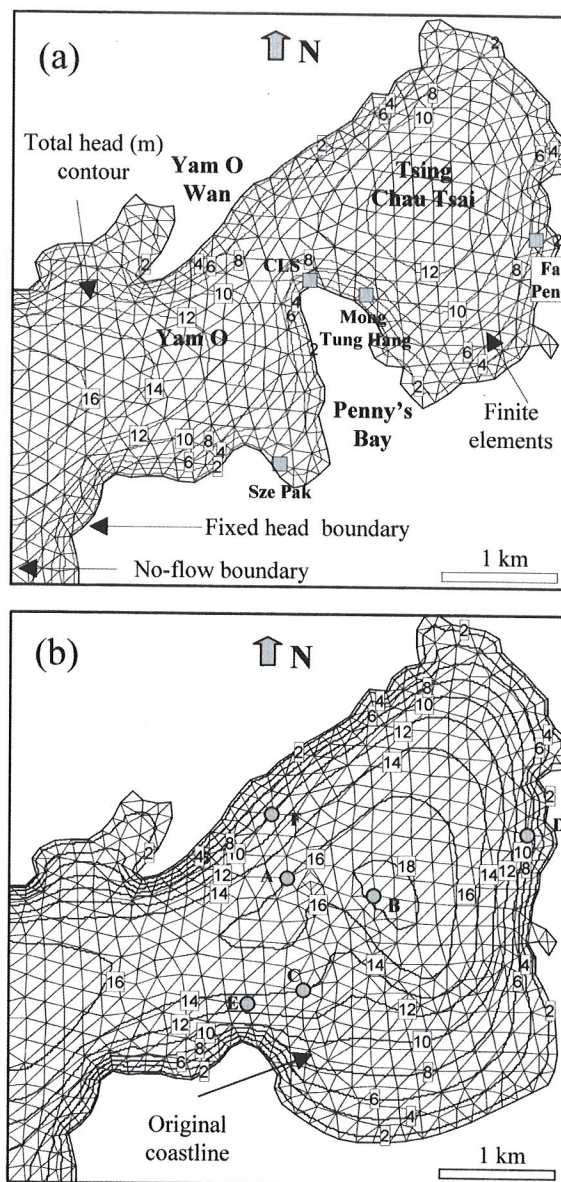


Fig. 2 Total groundwater head distributions in the land area around Penny's Bay before (a) and after (b) land reclamation

demonstrates that, if the possible impact of land reclamation on groundwater regimes is investigated in advance of the reclamation project, there are certain measures that can reduce the buildup of the water levels and the possible environmental and engineering consequences of land reclamation.

FEMWATER can output the boundary flux which provides information on the potential seepage rate along the coastline. Three portions of the coastline A-A', B-B' and C-C' (see Figure 3b) are chosen for detailed discussion. The results indicate that the seepage rate along the three portions of coastline would increase by 26%, 34%, and 26% respectively. Obviously, reclamation can



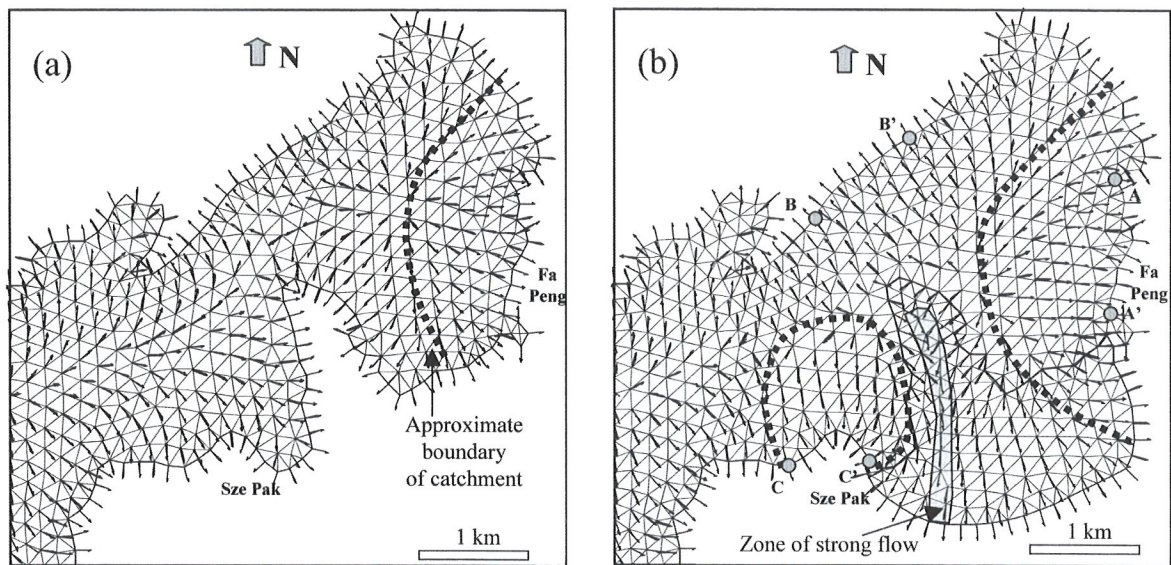


Fig. 3 Groundwater velocity distributions in the land area around Penny's Bay before (a) and after (b) land reclamation

lead to a significant increase in submarine groundwater discharge. The most significant increase along the coastline in the model is near Yam O Wan.

### Contaminant transport in response to reclamation

To understand how the contaminated groundwater below the CLS will transport and spread out after land reclamation, a transport simulation was carried out using FEMWATER. Some of the key transport parameters used for this simulation are listed in Table 1. Measurement of transport parameters is usually more uncertain than that for hydraulic parameters. In general, movement of contaminants is dominantly controlled by hydraulic parameters such as permeability and flow velocity (Zheng and Jiao, 1998).

In the model, a source with a concentration of 100% is added to a nodal point near the location of the CLS. The plumes after 5, 10, 50, and 100 years are presented in Fig. 4. After reclamation, the original site of the CLS is located at the groundwater divide (Figure 2b), where groundwater flow velocity is small. Consequently the plume does not seem to spread very far at the beginning. At about 50 years (Fig. 4c), the overall plume looks symmetrical, but it tends to spread more toward the coastal area, away from Penny's Bay. By about 100 years, the contaminated groundwater has reached the coastline near Yam O Wan, as shown by the contour for 5% contamination concentration. Although the CLS site is located at the coast of the original Penny's Bay, due to the groundwater flow pattern modified by the land reclamation, the contaminated

groundwater will not spread significantly within Penny's Bay. Instead, it travels northeast to areas away from the Bay.

### Possible engineering & environmental impacts of the land reclamation

It is well accepted that an increase in groundwater head will reduce slope stability. Therefore, slope stability will be affected in the areas where the total groundwater head is significantly increased. The areas with the most significant increase in head are the slopes near A, B, C (Fig. 2b). The slopes near B (Fig. 2) are most the vulnerable, since not only has the water level increased significantly but also the slopes are quite steep (Fig. 1). Drainage measures can be taken to reduce the groundwater level rise in these areas and minimise slope instability.

Attention should also be paid to areas beyond the vicinity of the reclaimed area. These locations are easily ignored, since most people do not generally link groundwater change with areas far from the reclamation site itself. Among the more distant slopes (near areas D, E, and F), the slopes near E or Sze Pak (Fig. 2b) would be of particular concern, since groundwater level there is significantly affected by the reclamation and the location has relatively steep slopes.

Groundwater seepage along the coastline is also altered by the reclamation. Some seepage in areas with low ground elevation may rise to become surface water, which will increase the chance of flooding in the case of heavy rainfall. A potential one third increase in groundwater discharge to the sea near Yam O Wan may impact on the quality



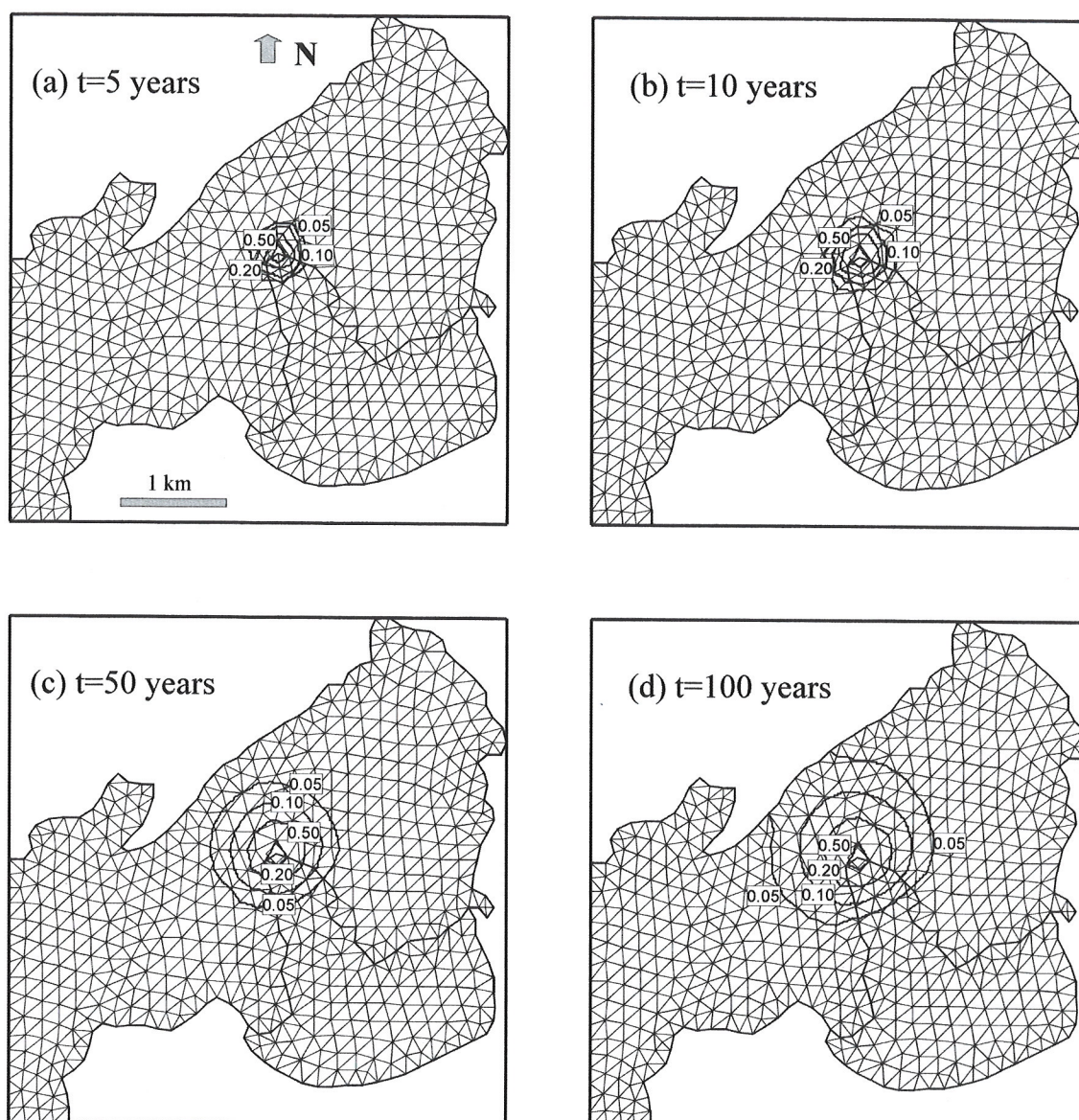


Fig. 4 Groundwater contaminant plumes at different times after reclamation (see text for discussion)

of the coastal waters. Contaminated soil should be fully removed and contaminated groundwater at the CLS needs to be pumped and treated. If it is not, then the contaminated groundwater will eventually travel beyond Penny's Bay and damage the coastal water quality near Yam O Wan. The modeled contaminated groundwater, however, does not appear to spread far within the Penny's Bay area.

### Limitations of the numerical simulations

The numerical simulation in this paper is not based on a real hydrogeological study of Penny's Bay and all the parameters have been assumed. None of the geological features such as fault zones and fracture network were considered. Furthermore, the aquifer system is assumed to be

unconfined, while in reality there may be confined groundwater along the fractured zone near the rockhead (Jiao and Nandy, 2001).

It should be noted that the model is run only for steady state. The entire system, including the background soil and the fill materials, is only divided into two layers. Each of these layers is assumed to be homogeneous and isotropic, while in reality both the background soil and the fill materials are heterogeneous.

The model assumes that rainfall recharge is uniform everywhere in the study area, but actually the recharge in the developed area will be much lower than in the natural area. It is also assumed that there is a clear-cut sea-land boundary and all the model layers are in perfect contact with the

seawater. The density difference between fresh groundwater and seawater is ignored.

In addition to the reclamation within Penny's Bay, there is also reclamation along the northern coast of Lantau, but this is not included in this study. The change in groundwater flow pattern and transport of contaminants would be therefore be much more complicated if all the geological, hydrogeological features, and other factors mentioned above were considered.

## Summary

This paper conducts numerical studies on the impact of land reclamation on a simplified groundwater flow system near Penny's Bay. The modeling results indicate that there would be a regional increase in total groundwater head after land reclamation. Change of the groundwater head is the most significant near the Bay, with a head increase of almost 200%. The areas beyond the Bay also have appreciable increase in groundwater head.

The change in the groundwater system is also reflected in submarine groundwater discharge. The area with the largest increase in submarine discharge is along the coast opposite to Penny's Bay. If the contaminant source at the CLS is not completely removed, the contaminated groundwater may eventually migrate to the coast of Yam O Wan and have an impact on the coastal water quality.

Attention should also be paid to the stability of the slopes in the areas within and beyond the reclamation area. A considerable water level rise may occur due to reclamation and the provision of drainage may be essential to manage this rising water level. The increase of seepage to the neighboring coast may have an impact on the coastal water quality. In low and flat areas, some seepage may reach the ground surface and increase the possibility of flooding during heavy rainfall periods.

This paper has also demonstrated that a hydrogeological study can help in the design of reclamation projects and the choice of placement locations for fill materials of different permeability. This can help in the management of the groundwater level and enable engineering impacts to be minimized. It should be pointed out that the detailed numbers used in this modeling study for the increase in water level and for travel time of the contaminants may not be realistic, since the model is not based on actual hydrogeological information. Nevertheless, it is believed the general conclusions about the change of the groundwater pattern and the overall contaminant spread are reasonable. Field

hydrogeological information and more comprehensive modeling studies are needed before more robust conclusions can be made.

## Acknowledgement

The study is partially supported by Hong Kong Research Grants Council grants: HKU 7105/02P and HKU CRCG. Professor Andrew Malone and Mr Tony Barriera read the manuscript and offered useful comments. Thanks also go to Mr Ding Guoping for his assistant in preparing diagrams.

## References

- Geotechnical Engineering Office (1993) *Guide to Retaining Wall Design (Geoguide 1) (Second edition)*. Geotechnical Engineering Office, Hong Kong, 297 p.
- Jiao, J. J. (2000) Modification of regional groundwater regimes by land reclamation, *Hong Kong Geologist*, 6, 29-36.
- Jiao, J. J and Nandy, S. (2001) Confined groundwater zone and slope instability in hillsides of weathered igneous rock in Hong Kong, *Hong Kong Geologist*, 7, 31-37.
- Jiao, J. J, S. Nandy, and Li, H. (2001) Analytical studies on the impact of reclamation on groundwater flow, *Ground Water*, 39(6), 912-920.
- Kwong, J.S.M. (1997) *A Review of Some Drained Reclamation Works in Hong Kong*. Geotechnical Engineering Office, Hong Kong, GEO Report No. 63, 53 p.
- Lin, H.J., Richards, D.R., Talbot, C.A., Yeh, G.T., Cheng, J.R., Cheng, H.P., and Jones, N.L. (1997) *FEMWATER: A Three-Dimensional Finite Element Computer Model for Simulating Density-Dependent Flow and Transport in Variably Saturated Media*, Technical Report CHL-97-12, U.S. Army Engineer Waterways Experiment Station, MS.
- Shen, C. K. and Lee, K. M. (1995) *Hydraulic Fill Performance In Hong Kong*, GEO Report No. 40, Geotechnical Engineering Office, Hong Kong.
- Zheng C. and Jiao, J. J. (1998) Numerical simulation of tracer tests in a heterogeneous aquifer, *J. Environmental Engineering*, 24(6), 510-516.

# Petrographical Features of Cataclasite: Evidence from the Lai Chi Kok-Tolo Channel Fault Zone, Hong Kong

Xiaochi Li<sup>1</sup> & Frank F.S. Woo<sup>2</sup>

1. Geotechnical Engineering Office, Civil Engineering Department, 101 Princess Margaret Road, Homantin, Kowloon, Hong Kong

2. Inter Pacific Limited, 21/F, Kiu Fu Commercial Bldg., 300 Lockhart Road, Wanchai, Hong Kong

## Abstract

Marginal deep faults of the "Lianhuashan Fault Zone" (LFZ) traverse the northwestern New Territories of Hong Kong, resulting in widespread occurrences of phyllitic and mylonitic rocks. In contrast, the Lai Chi Kok - Tolo Channel Fault Zone, an important second-order structure within the LFZ, is characterized mainly by brittle deformation resulting in cataclasite and cataclastic granite. These two dynamo-metamorphic rocks imply a totally different tectonic setting.

Cataclasite and cataclastic granite were recovered from boreholes in the Sha Tin area of Hong Kong. These occurrences provide direct evidence of movements along the Lai Chi Kok - Tolo Channel Fault Zone. Detailed petrographical features of the cataclasite are described, both in hand specimens and thin sections. The nomenclature and classification of the two major types of dynamo-metamorphic rocks is discussed, brittle deformation caused by elastic-friction mechanism, and plastic deformation characterized by dynamic re-crystallization.

## 摘要

香港的地質構造主要受到中國南部蓮花山斷裂帶的控制。蓮花山斷裂帶的北部邊界斷層切過香港新界的西北部，形成了大量糜棱岩、千枚岩等塑性構造變質岩。與此現象相反，脆性構造變質岩，如斷層角礫岩、碎裂岩等出現於荔枝角—赤門海峽斷裂帶內。該斷裂帶是香港境內最大規模的斷層之一。通過對沙田鑽孔中碎裂岩的詳細研究，包括岩石手標本的鑒定及薄片的鏡下觀察，討論了構造動力變質岩的分類及命名，指出兩種不同類型的構造變質岩的出現證明這兩個斷裂帶在性質上存在極大的差異。

## Introduction

The Sha Tin - Tolo Channel alignment contains complex geological structures, and is thus a key area in which to resolve some of the regional structural problems in Hong Kong. Burnett & Lai (1985) named this fault, an important secondary structure within the Lianhuashan Fault Zone, the "Lai Chi Kok—Tolo Channel Fault". The fault extends southwestwards from Mirs Bay in the northeast, passing along Tolo Channel and Ma On Shan, through Lai Chi Kok and to the south of Lantau Island (Fig. 1).

Cataclasite, which is one of the most important dynamo-metamorphic rocks (or tectonites), provides direct evidence for fault movement. However,

cataclasite has, so far, only been found in the Sha Tin area, within the inferred Lai Chi Kok - Tolo Channel Fault Zone. This paper presents the results of a detailed petrographical study of cataclasite samples collected from boreholes in Sha Tin.

The nomenclature and general classification of dynamo-metamorphic rocks is discussed, based on ductile and brittle deformation characteristics. Cataclasite samples from the Sha Tin area reveal features of brittle deformation caused by local faults. Crushing along this tectonic zone was subsequently followed by pronounced thermal alteration, including chloritization, epidotization and carbonation. The character of the rocks associated



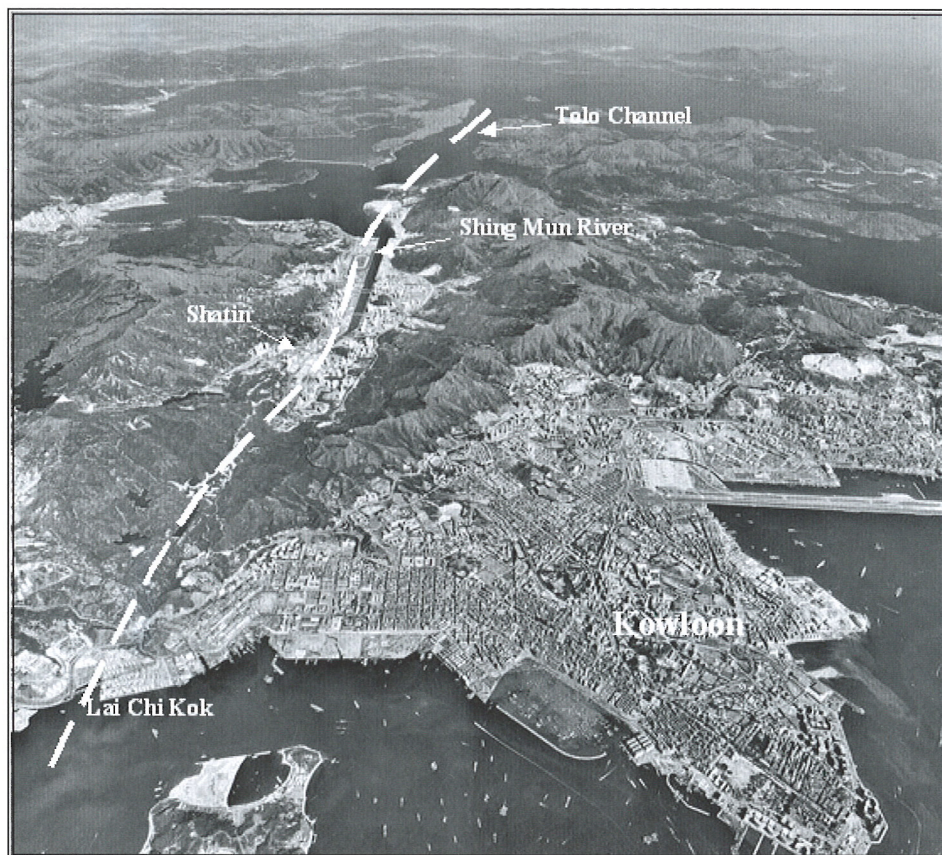


Fig. 1 Topography of the Lai Chi Kok - Tolo Channel Fault in Hong Kong

with the Lai Chi Kok - Tolo Channel Fault Zone differs markedly from the dynamo-metamorphic rocks in the northwest New Territories of Hong Kong, where ductile and brittle deformation resulted in the formation of phyllites and mylonites.

### Geology Revealed in the Boreholes

Cataclasites, and rocks with cataclastic textures, were found in four boreholes located at the northeastern corner of the Sha Tin KCR Station. This area, which used to be close to the tidal channel

of the Shing Mun River, was reclaimed in the 1970s for development of the Sha Tin New Town.

The general stratigraphy revealed in each of the boreholes is presented in Table 1. Cataclasite was encountered in three boreholes (BH3, BH5 and BH8), and cataclastic granite was observed in one borehole (BH6). Unfortunately, because of the inferred steeply inclined or nearly vertical dip of the fault plane, none of the boreholes completely penetrated the tectonic zone.

	BH 3	BH 5	BH 6	BH 8
<b>FD</b>	0.00-5.05m	0.00-3.05m	0.00-7.10m	0.00-5.10m
<b>MD</b>	5.05-9.85m	—	—	—
<b>AD</b>	9.85-12.80m	3.05-5.55m	7.10-10.60m	5.10-8.40m
<b>CDR</b>	12.80-33.80m	5.55-19.00m	10.60-16.90m	8.40-16.75m
<b>FrR</b>	33.80-42.66m	19.00-28.58m	16.90-22.30m	16.75-28.19m
<b>R-Type</b>	<b>Cataclasite</b>	<b>Cataclasite</b>	<b>Cataclastic Granite</b>	<b>Cataclasite</b>
<b>FD</b> — recent fill <b>MD</b> — marine deposit <b>AD</b> —Alluvium <b>CDR</b> — completely decomposed rock <b>FrR</b> — fresh rock <b>R-Type</b> — rock type				

Table 1 - Borehole data



## Petrographical Features of the Cataclasite in Hand Specimen

Emphasis is given to a discussion of the petrographical features of the cataclasite in hand specimen, omitting the cataclastic granite.

### General Rock Description

The samples were predominantly a light pinkish grey to pale yellowish grey, becoming greenish grey if chloritization or epidotization was present. Dark brown dappling or streaking was observed on some specimens. Observed textures included cataclastic, porphyroclastic, and blastotaxitic. Banded structures were also present.

### Mineralogy

Mineralogically, the rocks consisted predominantly of feldspar and quartz, with some muscovite, epidote, chlorite and carbonate, as well as minor pyrite and sericite.

**Feldspar:** constituted about 50% of the total rock-forming minerals in the samples. Feldspar occurred as light pinkish to pale yellow, irregularly shaped crystals. The majority were crushed or deformed, and observed infilling the interstices between quartz grains. Most feldspars were either partially weathered, or altered to kaolin.

**Quartz:** constituted about 45% of the minerals. The majority of the quartz was grey in colour, and irregularly granular with typical porphyroclastic textures. Crush textures, fractured rims and fragmented outer rims were well developed.

**Epidote & Chlorite:** constituted about 3-5% of the minerals. They were light to dark green in colour, occurring as infilling in the cataclastic cracks, or scattered throughout the rock.

**Carbonate:** constituted less than 1%. The carbonate was white in colour, occurring as infilling in the cataclastic cracks, or as a thermal replacement of other minerals.

**Muscovite, Sericite and Pyrite:** occurred as minor minerals, scattered along altered bands or as infillings in cracks. Usually occurred in association with chlorite.

### Textures and Structures

The samples from boreholes BH-3, BH-5 and BH-8 showed typical cataclastic textures (Fig. 2). Fine strain cracks were well developed in the quartz grains, which usually occurred in association with fractured outer rims. Feldspar crystals were observed to be highly deformed and crushed (probably also altered or decomposed), commonly filling the interstices between

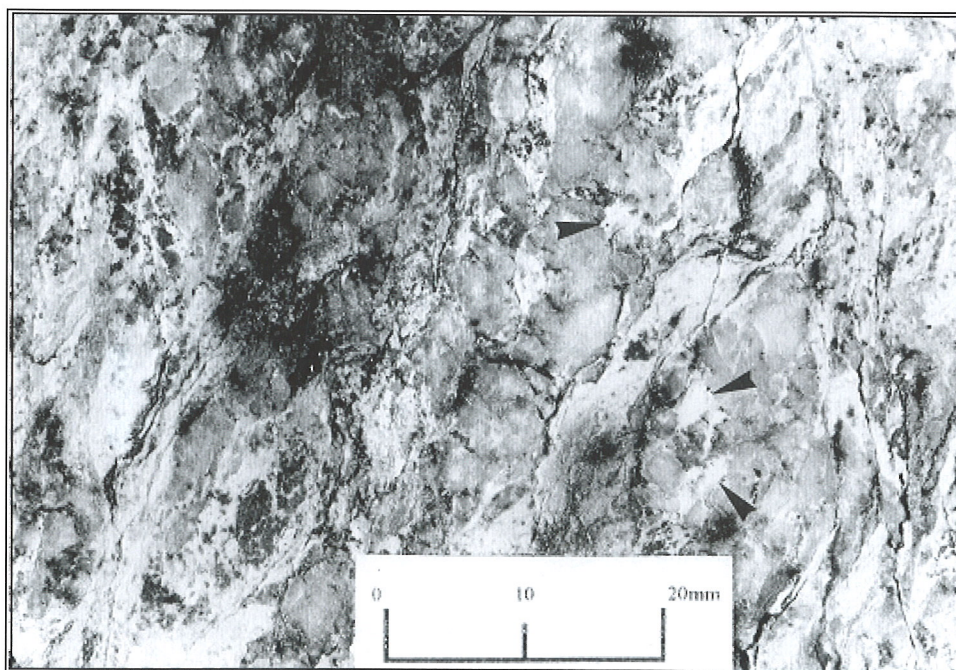


Fig. 2 Cataclasite: HK12086 Locality: BH-3 Shatin. Typical cataclastic texture with well-developed crush cracks. The grey grains are quartz and the white are feldspar. Note the micro-cracks in the quartz; tiny broken grains of quartz are partially oriented. Dark stains are epidote and chlorite. The arrows point to the thermal carbonate.



quartz grains. The quartz was strongly squeezed and crushed. Original quartz crystals had been totally destroyed (Fig. 3). Chlorite was seen to be lining cracks or filling the interstices between finely broken grains of quartz and feldspar. Also noticeable was a broad orientation or alignment of the minerals in the fabric, reflecting the strong pressures to which the rocks had been subjected.

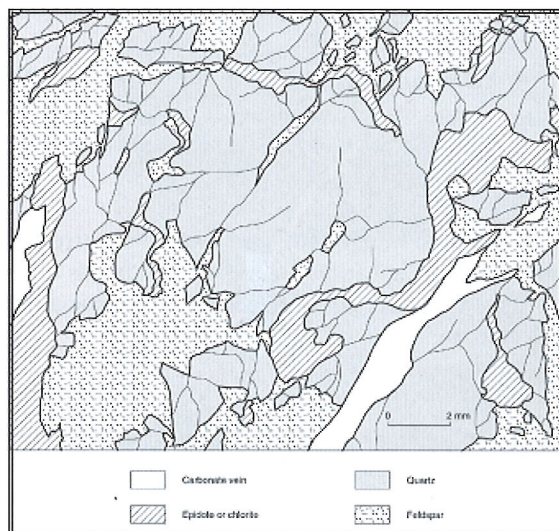


Fig. 3 Cataclasite: HK12086(B) Locality: BH-3 Shatin. Original grains of feldspar and quartz that have been destroyed in cataclasite

The sample from BH-6 showed a relict granitic texture, but with well developed micro-cracks and crush fissures (Fig. 4). Based on the identified deformation features, especially the porphyroclastic or mortar textures, these rocks should be classified as "cataclastic granite". Thrush (1968) used the term "haplophyre" to name similar porphyroclastic granite in the European Alps.

### Micro-Textures of Cataclasite and Cataclastic Granite

Several features were identified more certainly in thin sections. In particular, cataclastic textures, especially the porphyroclastic texture, weathering and alteration features on grains of feldspar were clearly seen under the microscope.

Well-developed micro-cracks were observed in the quartz grains. Quartz grains were commonly crushed, and an undulatory extinction was noted. The cracks were filled with cataclastic powders consisting of comminuted quartz mixed with very fine sericite, which is probably an alteration product of feldspar. The powders had a grain size of about 0.001mm to 0.05 mm.

The most intensive cataclasis was recognized in samples from boreholes BH-3, BH-5 and BH-8. Thin sections showed that most of the rock-forming minerals (notably feldspar and quartz) were broken into constituent grains, although relict granitic textures were

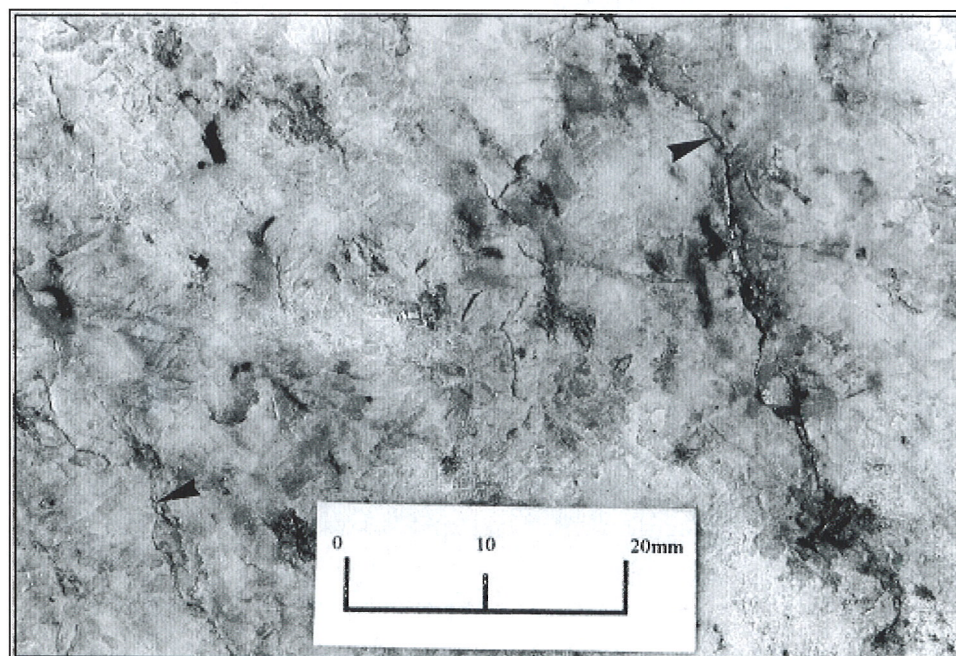


Fig. 4 Cataclastic Granite: HK12089 Locality: BH-3 Shatin. Relict granitic textures with indistinct boundaries between the mineral grains. Dark stains are epidote and chlorite. Note the micro-cracks in both the feldspar and quartz grains. The arrows point to crush fissures.



recognized locally. The interstices of the porphyroclasts were filled with cataclastic powder (Fig. 5), which in some cases were cemented by carbonate or ferromanganese minerals.

Well-developed cataclastic textures imply typical brittle deformation by dynamo-metamorphism. Cataclastic flow textures were seen in some sections of the samples. These textures are formed by strongly oriented cataclastic powders, which consist of broken quartz, feldspar, muscovite, and sericite (Fig. 6). They can be regarded as a transitional texture between brittle and plastic deformation, which indicates high stress or shearing conditions.

## Classification of Dynamo-metamorphic Rocks

Dynamo-metamorphic rocks, such as phyllite, mylonite and cataclasite are termed tectonites. The earliest research on tectonites was carried out by Lapworth nearly a century ago on rocks collected from the Moine Thrust Fault in Scotland (Zhong & Guo, 1991). Subsequent field and laboratory research has improved the classification of tectonites. During the 1970s, a breakthrough in the study of rock deformation resulted in a new understanding of their origins. Mylonites, phyllites, phyllonites and related rocks have

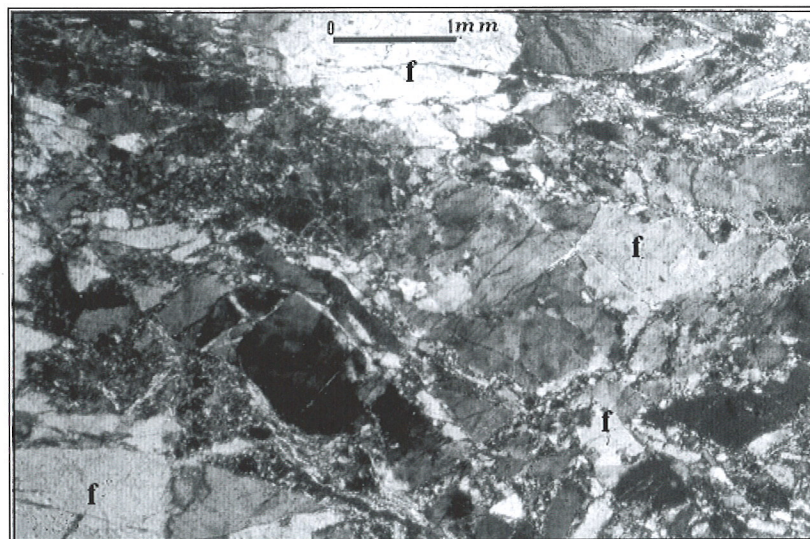


Fig. 5 Cataclasite: HK12088 Locality: BH-3 Shatin. Cataclastic texture under the microscope. Note the micro-cracks in the quartz grains (grey to dark grey, or black) and the feldspar grains (marked "f"). Crush fissures are filled with cataclastic powders.

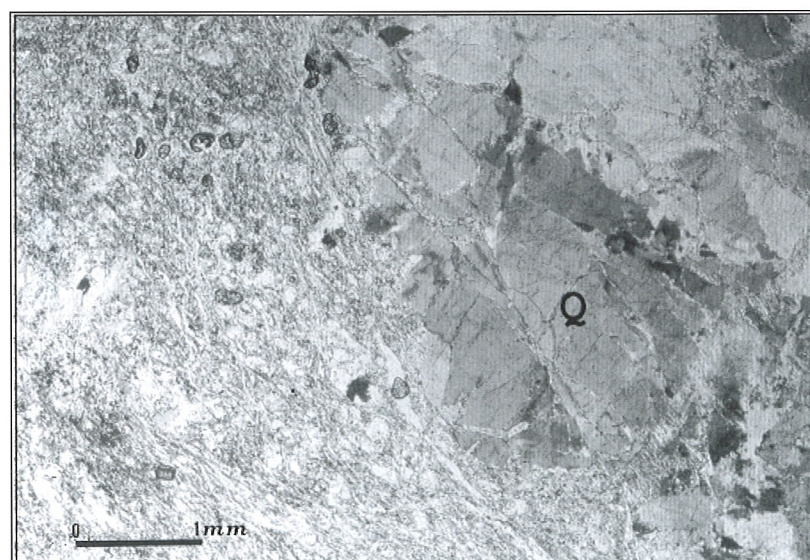


Fig. 6 Cataclastic Flow Texture: HK12088(B) Locality: BH-3 Shatin. Typical cataclastic flow texture. Note the difference in grain size between the quartz grains (marked "Q") and flow materials. Note the micro-cracks in the quartz grains.



Deformation		Brittle Deformation		Plastic Deformation				
Textural Features	Cataclastic Brecciated Texture (Grain size >2mm)	Cataclastic Texture (Grain size 0.05-2mm) Percentage of Matrix:		Flow Texture % of Matrix Materials:				Submicroscopic granular/glass
		<50%	>50%	<10%	10-50%	50-90%	>90%	
Rock Type	Tectonic Breccia	Cataclastic Rocks	Cataclasite	Mylonitic Rocks	Pre-Mylonite Schist	Mylonite Phyllite	Ultramylonite Phyllonite	Pseudotachylite

Table 2 Classification of rock deformation (After Zhong &amp; Guo, 1991)

been separated from fault breccias and cataclasites according to the deformation mechanism. It is now accepted that mylonites and phyllites, which are characterized mainly by dynamic re-crystallization, result from plastic deformation and not from the grinding of brittle materials.

Sibson (1977) proposed a model of tectonite formation that included two series of rocks, cataclasites formed by an elastic-friction mechanism, and mylonites resulting from a plastic strain mechanism. Subsequently, Zhong & Guo (1991) produced a simplified classification of dynamo-metamorphic rocks based on rock deformation mechanisms (Table 2). This scheme is widely adopted. According to this classification, the Sha Tin samples fall into the categories of cataclasite or cataclastic granite.

#### Implications of Cataclasites

All dynamo-metamorphic rocks, produced by both plastic and brittle deformation, are the result of tectonic movements. They are, therefore, direct evidence of tectonic activity. The elastic-friction mechanism is usually confined to shallow depths in the Earth, and results in brittle deformation. Plastic strain mechanisms occur at deeper levels and result in the ductile deformation of rocks. The critical depth separating these two mechanisms is about ten to fifteen kilometres below the surface (Zhong & Guo, 1991).

Qiu (1992) established a two-layer model of the continental marginal fractures in Guangdong Province. A series of deep faults in the Province reflected southeastwards shearing-slipping of the Upper Crust along the basement gliding plane. With depth, the rock deformation patterns changed from brittle to ductile and the steep fault planes become more gently inclined. The study concluded that the Yanshanian regional tectonic movements in South China comprised an earlier (Jurassic) faulting, categorised as imbricate nappe structures showing mainly ductile deformation, and later (Cretaceous) structures, exhibiting brittle fractures of a steep thrust.

In Hong Kong, both brittle and plastically deformed rocks have been found. In addition to cataclasite from Sha Tin, some typical plastically deformed rocks, including mylonites and phyllites (Fig. 7) have been mapped over a wide area of the North and Northwest New Territories of Hong Kong. These rocks represent different geological settings and were formed by different tectonic mechanisms.

The geology of Hong Kong is principally controlled by the Lianhuashan Fault Zone (LFZ) of South China, which consists of up to 120 parallel faults of the order of 20-40 kilometres wide (Fig. 8). The Bureau of Geology and Mineral Resources of Guangdong Province (BGMRGD, 1988) recognized two major parallel marginal deep-fault groups in the LFZ. These control

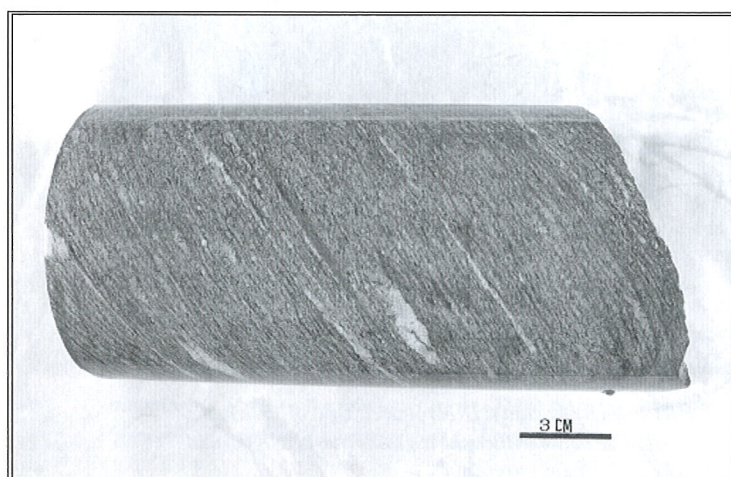


Fig. 7 Phyllite (foliated tuff): HK12101  
Locality: Ng Tung River, Northwest New Territories.



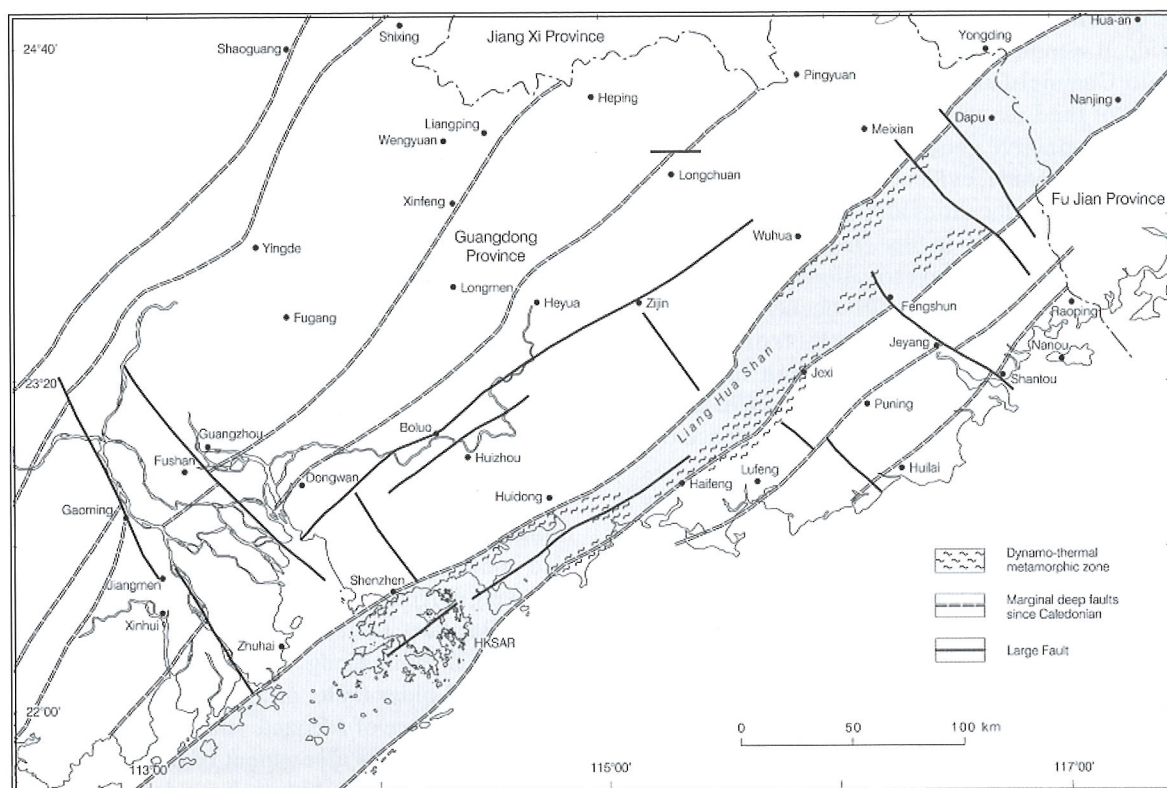


Fig. 8 Simplified Map of the Lianhuashan Fault Zone and Deep Faults since the Caledonian (After BGMRC, 1988)

both sides of the LFZ and exhibit typical features of a ramp structure:

**Southeast Group:** occurring southeast of Lianhuashan, striking  $040^{\circ}$ - $050^{\circ}$  and dipping SE with dip-angles of  $40^{\circ}$ - $70^{\circ}$

**Northwest Group:** occurring west of Lianhuashan, striking  $030^{\circ}$ - $050^{\circ}$ , and dipping NW with dip-angles of  $40^{\circ}$ - $85^{\circ}$

Ding & Lai (1997) noted that "Hong Kong is bounded by the northeast-trending Shenzhen and Haifeng faults that define the NW and SE boundaries respectively of the Lianhuashan Fault Zone". Along these marginal deep faults, silicification, mylonitization, schistosity, cleavage, tectonic block-lenses and dynamo-thermal metamorphism are well developed. Exposures of plastically deformed rocks, produced by deep faulting, have been recorded in several localities in Guangdong Province (Fig. 8).

The foliated tuffs and sedimentary rocks, phyllites and mylonites, in the northwestern New Territories are probably associated with the north marginal fault (the Shenzhen Fault) of the LFZ. This fault, which is characterized by plastic deformation, implies a more intensive tectonic movement. In contrast, the cataclasite from Sha Tin provides evidence of a second-order structural feature within the LFZ.

The fault is shallower than the deep marginal faults and is characterized mainly by brittle deformation. Although the fault in Sha Tin may not be considered a major fault in South China, locally it is a principal fault.

### The Lai Chi Kok - Tolo Channel Fault

Bennett (1984) pointed out that, in Hong Kong, "the dominant structures trend NE and NW. The NE faults are the more prominent and can be related in general terms to the major structures mapped in southern China". Burnett & Lai (1985) described the Lai Chi Kok - Tolo Channel fault, pointing out that ".....this fault begins at Bluff Head and may be traced along the north coast of Tolo Channel to Sha Tin and Lai Chi Kok.....field mapping in the vicinity of Sha Tin has established the local attitude of the fault as  $040^{\circ}$ - $050^{\circ}$  /  $70^{\circ}$ - $80^{\circ}$  (strike/dip angle).....Along the fault, a compressive crushed zone was formed which consists of cataclasite, fault breccia and gouge with accompanying intensive kaolinization and chloritization.....on both sides of Tolo channel a fault-scarp shoreline with triangular facets occurs. The fault appears to control the distribution of the local Palaeozoic strata, forming some narrow tectonic lenses, the strata being very steep or even overturned within the fault zone". Chen (1987) later described this fault, considering it as one of the principal sets within the LFZ.

Since the area affected by this fault is very wide, it is more appropriate that the "Lai Chi Kok – Tolo Channel Fault" is considered as a sub-fault zone of the Lianghuashan Fault Zone. In addition to the distinctive geomorphological features along the Tolo Channel, evidence of this fault can also be found in many localities along the Shing Mun River Channel, especially in Sha Tin area.

Previous site investigations record shattered and highly fractured granite occurring along the Shing Mun River Channel (from Sha Tin northeastwards past Ma On Shan to the Tolo Channel, and southwestwards to Lai Chi Kok and beyond), providing direct material evidence of the Lai Chi Kok – Tolo Channel Fault.

Information from ground investigations in the Ma On Shan Reclamation Area shows a broad (10-100m wide) NE-trending fault zone. According to Sewell (1996) "The fault zone has been intersected at depths ranging from 40 m to at least 120 m below ground surface, and comprises highly sheared rock, mineralized and hydro-thermally altered deposits and soft fault gouge, and thick, mixed colluvium and debris flow deposits. Fractured marble is encountered on the northern margin of the fault zone together with iron-mineralized and hydrothermal deposits".

A recent offshore magnetic survey (EGS, 1999) revealed a distinctive NE-trending magnetic anomaly zone, indicating the southwesterly extension of the Lai Chi Kok-Tolo Channel Fault. The anomaly indicates an offshore continuation of the fault. Further, cataclastic granite with phyllosilicates and fault gouge was encountered in tunnels in this area (Merriman *et al.*, 1998). These rocks probably relate to, or at least have been affected by, movement upon the Lai Chi Kok – Tolo Channel Fault.

The recent discovery of dynamo-metamorphic rocks from boreholes in Sha Tin provides further confirmatory evidence for the existence of this fault.

## Wider Considerations: A Brief Review of Regional Tectonics

The LFZ is one of the main post-Caledonian regional deep faults in South China. It is an important boundary structure for regional tectonic subdivisions in Guangdong Province. The LFZ zone extends northeastwards over several hundred kilometres along the Lianghuashan passing through Jexi, Fengshun, and Dapu in Guangdong Province, into the area of Nanjing and Hua-an in Fujian Province. Southwestwards, it passes through

Haifeng, Huidong, and Shenzhen, before crossing into the South China Sea (Fig. 8). Since the Indosinian Movements, the LFZ has had a long history of multiple cycles of movement. These movements have influenced the erosion of the Late Palaeozoic strata in southern China, and controlled magmatic activities and the distribution of sedimentary processes during the Mesozoic.

The geology of Hong Kong has also been controlled by the evolution of the LFZ. During the Mesozoic period in Hong Kong, as in southern China, the environment was characterized by cycles of multiple-centred, repeated and intermittent volcanic eruptions, and subsequently by the accompanying emplacement of magmatic intrusions. The fault zone not only formed an important transverse structure for magmatic injection, but it also controlled the pattern of tectonic movements following magmatism.

Bennett (1984) pointed out that many structures in Hong Kong "almost certainly represent rejuvenated older faults or zones of weakness, but given the absence of adequate stratigraphical or time markers, a rigorous assessment of their movement histories is difficult". Although the detailed history of the Lai Chi Kok-Tolo Channel Fault has not been determined, because of its strong topographical imprint and NE trending orientation it can be concluded that this fault has inherited the tectonic orientation of previous structures in the LFZ, and is one of the most important secondary structures within the zone.

A model of crustal structure in Hong Kong has been established based on gravity data supported by isotopic analysis (Fletcher *et al.*, 1997). A north-south profile across Hong Kong (close to Lai Chi Kok) shows a triformed middle to lower crustal structure (Fig. 9) "a narrow, NE-trending, felsic segment flanked by more mafic segments, which are considered to represent Archaean and Proterozoic terranes respectively. These are overlain by an upper crustal element, approximately 6 km thick, composed of Mesozoic granitic and volcanic rocks and Phanerozoic strata" (Fletcher *et al.*, 1997). The Lai Chi Kok-Tolo Channel Fault is interpreted as a Mesozoic or post-Mesozoic tectonic structure that developed only in the upper crustal element, because it is distinctively characterized by brittle deformation. Although this important fault represents rejuvenated older tectonic zones of weakness, there is no evidence to show that the fault penetrates to middle and lower crustal elements. It may be the essential criteria to distinguish it from the marginal deep faults, which resulted in the formation of phyllites over large areas of the northwestern New Territories of Hong Kong.



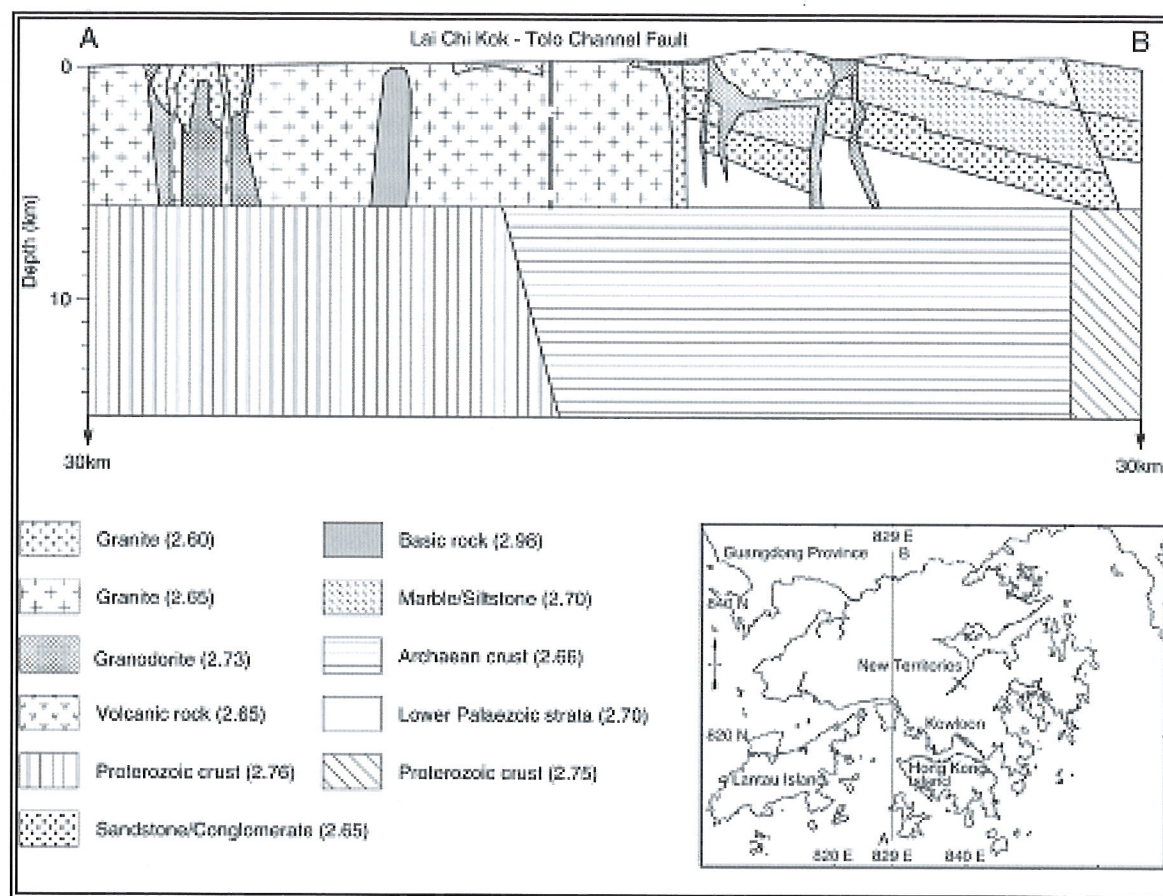


Fig. 9 Crustal Structure Model of Hong Kong (after Fletcher et al., 1997) (Figs. in brackets indicate rock density)

## Conclusions

1. Evidence for both the marginal deep faults of the Lianhuashan Fault Zone and second-order structures within LFZ have been discovered in Hong Kong, reflecting different mechanisms. The former is characterized by plastic deformation, whereas the latter exhibits features of brittle deformation.

2. Rock samples from drillholes in the Sha Tin area show a typical cataclastic texture. These lithologies should be considered as the most important direct evidence for the presence of the Lai Chi Kok - Tolo Channel Fault.

3. Cataclastic rocks, formed by an elastic-friction mechanism, exhibit features of brittle deformation that indicate tectonic movements in the upper part of the Upper Crust (less than 10 kilometres in depth). Rocks of the Lai Chi Kok - Tolo Channel Fault contrast markedly with those of the marginal deep faults of the northwestern New Territories of Hong Kong.

4. Phyllites and mylonites occur over large areas of the northern and northwestern New Territories of Hong Kong. These rocks result from

plastic strain mechanisms, a feature of stronger dynamo-metamorphism. These lithologies should be regarded as the products of the deep marginal faults of the LFZ.

## Acknowledgments

This paper is published with the permission of the Head of the Geotechnical Engineering Office and the Director of Civil Engineering of the Government of the Hong Kong Special Administrative Region. The authors would like to thank Dr. Raynor Shaw for his valuable editorial assistance in revising the manuscript. Comments by Professors Yang Zunyi and Jin Shuyan of China University of Geosciences are greatly acknowledged.

## References

- Addison, R. (1986) *The Geology of Sha Tin. Hong Kong Geological Survey Memoir No. 1*, Geotechnical Control Office, Civil Engineering Services Department, Hong Kong Government, 85p.
- Allen P. M. & Stephens, E.A. (1971) *Report on the Geological Survey of Hong Kong*. The Government Printer, Hong Kong, 107p.
- Argon Geochronology Laboratory of The University of Toronto (2000) *<sup>40</sup>Ar–<sup>39</sup>Ar Laser Microprobe Dating of Samples from Hong Kong: Phase III: Fault Rocks HK3419, HK7284, HK7729, HK12077, HK12078 and HK12086*. 42p.
- Bennett, J. D. (1984) *Review of the Tectonic History, Structure and Metamorphism of Hong Kong. GCO Publication 6/84*, Geotechnical Control Office, Hong Kong Government, 63p.
- Burnett, A. D. & Lai, K. W. (1985) A Review of the Photogeological Lineaments and Fault System of Hong Kong. Geological Aspects of Site Investigation, *Geological Society of Hong Kong Bulletin*, No. 2, 113-131.
- BGMRGD (1988) *The Regional Geology of Guangdong Province*. Geological Memoir Series 1, Number 9, Bureau of Geology and Mineral Resources of Guangdong Province, Ministry of Geology and Mineral Resources, People's Republic of China, Geological Publishing House, Beijing, 941p. (in Chinese with English abstract)
- Chen, T. G. (1987) Basic Features of the Lian Hua Shan Fault Zone in the Hong Kong and Shenzhen Area. *Journal of Guangdong Geology*, 2 (2), 57-68 (in Chinese).
- Ding, Y. Z. & Lai, K. W. (1997) Neotectonic Fault Activity in Hong Kong: Evidence from Seismic Events and Thermoluminescence Dating of Fault Gouge. *Journal of the Geological Society, London*, 154(6), 1001-1007.
- EGS (1999) *Green Island, Tsing Yi and Peng Chau Magnetic Survey: Preliminary Report*. Contract Number GE/97/12, Job Number HK132898, Electronic and Geophysical Services (Asia) Limited, 7p (with 5 figures).
- Fletcher, C. J. N., Campbell, S.D.G., Carruthers, R.M., Busby, J.P. & Lai, K.W. (1997) Regional Tectonic Setting of Hong Kong: Implications of New Gravity Models. *Journal of Geological Society, London*, 154(6), 1021-1030.
- Lai, K.W. & Langford, R.L. (1996) Spatial and Temporal Characteristics of Major Faults of Hong Kong. Seismicity in Eastern Asia, *Geological Society of Hong Kong Bulletin*, No. 5, pp 72-84.
- Merriman, R.J., Kemp, S.J. & Hards, V.L. (1998) *The Mineralogy and Petrography of Fault Rocks Beneath the Western Harbour, Hong Kong*. British Geological Survey Technical Report WG/98/40C, Mineralogy & Petrology Series, 8p.
- Qiu, Y.X. (1992) Regional Tectonic Evolution and its Basic Features in Guangdong Province. *Guangdong Geology*, 7 (1), 1-26 (in Chinese with English abstract).
- Ruxton, B.P. (1957) The Structural History of Hong Kong. *Far Eastern Economic Review*, No. 23, 783-785
- Ruxton, B.P. (1960) The Geology of Hong Kong. *Quarterly Journal of the Geological Society of London*, 115, 233-260.
- Sewell, R.J. (1996) *Geology of Ma On Shan. Hong Kong Geological Survey Sheet Report 5*, Geotechnical Control Office, Civil Engineering Services Department, Hong Kong Government, 45p.
- Sewell, R.J. & Campbell, S.D.G. (1998) *Absolute age-dating of Hong Kong volcanic and plutonic rocks, superficial deposits, and faults*. GEO Report No. 118, Geotechnical Engineering Office, Civil Engineering Department, The Government of the Hong Kong SAR, 42p.
- Sewell, R.J., Campbell, S.D.G., Fletcher, C.J.N., Lai, K. W. & Kirk, P.A. (2000) *The pre-Quaternary Geology of Hong Kong*. HK Geological Survey, Geotechnical Engineering Office, Civil Engineering Department, The Government of the Hong Kong SAR, 181p.
- Sibson, R.H. (1977) Fault rocks and Fault Mechanisms. *Journal of the Geological Society, London*, Vol. 133, pp 191-213.
- Wong, K.M. & Ho, S. (1986) Dolomitic Limestone in Tolo Harbour. *Geological Society of Hong Kong Newsletter*, 4(4), 20-23.
- Zhong, Z.Q. & Guo, B.L. (1991) *Tectonites and Microtextals*. Publishing House of the China University of Geosciences, Wuhan, 128p. (in Chinese).

## The Lai Chi Chong Section: A Photographic Feature

S.D.G. Campbell and R. Shaw

Hong Kong Geological Survey, Geotechnical Engineering Office, Civil Engineering Department, 11/F Civil Engineering Building, 101 Princess Margaret Road, Ho Man Tin, Kowloon, Hong Kong.

### Abstract

Exposures along the coastal rock platform at Lai Chi Chong, on the southern shores of the Tolo Channel, reveal a wide range of soft sediment structures that are arguably without parallel in Hong Kong. Representative features are illustrated and described, with the aims of further highlighting this important geological locality, which is a Site of Special Scientific Interest, to the local geological community, encouraging student field studies, and emphasizing the importance of the site in the hope that research to unravel the full complexities of the geological history will be stimulated. Visitors to the site must, however, respect the need to preserve the site for the benefit of future generations.

### 摘要

赤門海峽南岸荔枝莊一帶的岩石露頭展示了各種類型的沉積岩柔性變形構造，這一地質現象是香港絕無僅有的。本文以大量圖片描述了該地具代表性的構造特征。其目的，是爲了向本埠的地質界特別推薦這個重要的特殊地質觀察點，並鼓勵學生們到該地進行野外學習，爲徹底解開這一地質歷史中複雜地質現象的來龍去脈而努力。到該地進行研究的人應注意爲後人保護這些地質構造的自然狀態。

### Introduction

Lai Chi Chong is situated on the southern shoreline of the Tolo Channel, in the north-east New Territories of Hong Kong. At low tide, the exposed rock platform around the coast is an excellent venue for geological field studies and has been designated as a Site of Special Scientific Interest (SSSI) under the responsibility of the Agriculture, Fisheries and Conservation Department. This locality conveniently allows the examination of a range of sedimentary structures, particularly soft sediment deformation structures. Because granitic and volcanic rocks underlie the majority of the terrain in the territory, opportunities to examine clearly identifiable sedimentary structures are rare. Consequently, these exposures are an extremely valuable educational asset for Hong Kong. Indeed, the sedimentary features exposed at Lai Chi Chong are considered to be of international importance.

### The Lai Chi Chong Formation

The rock platform around the coast at Lai Chi Chong displays the type section of the Lai Chi Chong Formation. The formation comprises a well-bedded succession of pale grey cherty tuffite, coarse ash crystal tuff, thin eutaxitic fine ash tuff, flow-banded porphyritic rhyolite, conglomerate, tuffaceous sandstone, and dark grey laminated silty mudstone (Sewell *et al.*, 2000).

Individual beds vary typically from 0.1 m to 6 m thick, and the complete Formation is from 130 m to 180 m thick.

Strange *et al.* (1990) first described the formation, regarding it as a single unit extending northwards from Three Fathoms Cove to Lai Chi Chong. However, subsequent U-Pb age-dating (Campbell & Sewell, 1998; Sewell *et al.*, 2000) has suggested that the formation should be restricted to the upper part of the succession.

The thicker tuffaceous sandstones and coarse ash tuffs contain silty mudstone intraclasts, flame structures, load casts, and other features characteristic of soft sediment deformation. These features are indicative of rapid emplacement by mass flow (low and high concentration turbidites and debris flows) onto unconsolidated sediments. Intra-formational slump folds are also common, many of which are large. Related syn-sedimentary faults and dewatering structures are additional evidence that the substrate was unconsolidated during deposition (Sewell *et al.*, 2000).

Terrestrial palaeontological remains are a feature of the formation. However, no marine fossils have been found. Thus, Strange *et al.* (1990) observed organic structures of possible algal origin in indurated dark grey siltstones. Several workers have described fossil plant fragments (including conifers and cycadophytes) and portions of tree-trunks from the type locality. These

suggest either a Jurassic age (e.g. Williams, 1943; Nau, 1986) or an Early Cretaceous age (e.g. Dale & Nash, 1984; Wai, 1986; Atherton, 1989; Lee *et al.*, 1997). Recently, a high precision U-Pb single crystal zircon age from near the top of the formation yielded an age of 146.2  $\pm$  0.3 Ma (reported in Sewell *et al.* (2000)) indicating a latest Late Jurassic age. This discrepancy has still to be resolved.

### The Lai Chi Chong Coastal Section

The coastal section that is well-exposed at Lai Chi Chong has long held the interest of geologists in Hong Kong. The observed folding and faulting have generally been attributed to local syndepositional processes (e.g. Strange *et al.*, 1990; Workman, 1991).

### Previous Descriptions and Interpretations

In the light of recent developments of the understanding of the stratigraphy in this area, this photofeature presents a set of field photographs that illustrate a range of sedimentary and structural features clearly visible in the rocks. These contributions are intended to supplement the excellent illustrations and accompanying map of the section presented by Workman (op. cit.). The structures illustrated and described here are useful guides to the environments in which the sediments were deposited, and the conditions under which they were deformed and fractured. However, it is emphasized that these interpretations are preliminary, and in some cases speculative. There is clearly a need, therefore, for a systematic and rigorous sedimentological and structural review of this important stratigraphical section.

### Soft Sediment Deformation Structures

The sedimentary features visible in the Lai Chi Chong Formation indicate that the beds accumulated in a volcanic environment, probably as lacustrine volcanoclastics deposited in a crater lake, or fault-controlled lake within an active volcanic region. Depositional sedimentary features such as normally graded bedding, flame structures, loading structures and convolutions indicate that, despite the high volcanoclastic component of many of the beds, the majority were of secondary sedimentary, and typically mass flow origin within a dynamic and unstable environment. However, some beds could be of a primary volcanic airfall origin, and possibly even volcanic surge origin, albeit deposited through a water column. A palaeoslope towards the south is suggested by several features including asymmetrical flame structures and asymmetrical conjugate fold sets. Intraformational folding suggests that several beds were possibly subject to volcanic eruption-related seismic disturbance, causing them to slide and deform, or in some cases fracture and imbricate.

### Acknowledgements

This paper is published with the permission of the Head of the Geotechnical Engineering Office and the Director of Civil Engineering of the Government of the Hong Kong Special Administrative Region. All the original photographs used in this paper were taken by Lloyd Homer, New Zealand, for the Geotechnical Engineering Office, Civil Engineering Department.

### References

- Atherton, M.J. (1989) Palaeontologists from the Nanjing University Institute of Geology and Palaeontology: Recent Fossil Finds in Hong Kong. *Geological Society of Hong Kong Newsletter*, 7, 42-43.
- Bouma, A.H. (1962) *Sedimentology of Some Flysch Deposits: A Graphic Approach to Facies Interpretation*. Elsevier, Amsterdam, 168p..
- Campbell, S.D.G. & Sewell, R.J. 1998. A Proposed Revision of the Volcanic Stratigraphy and Related Plutonic Classification of Hong Kong. *Hong Kong Geologist*, 4, 1-11.
- Dale, M.J. & Nash, J.M. (1984) The Occurrence of Silicified Wood in the Repulse Bay Formation Sediments at Lai Chi Chong, New Territories, Hong Kong. *Geological Society Hong Kong Newsletter*, 2, 1-4.
- Lee, C.M., Chan, K.W. & Ho, K.H. (1997) *Palaeontology and Stratigraphy of Hong Kong: Volume 1*. Science Press, Beijing, 206p. plus 57 plates.
- Nau, P.S. (1986) Discussion on the Age of the Rock Sequence on the Coast North of Lai Chi Chong, New Territories, Hong Kong. *Geological Society of Hong Kong Newsletter*, 4, 1-4.
- Sewell, R.J., Campbell, S.D.G., Fletcher, C.J.N., Lai, K.W. & Kirk, P.A. (2000) *The Pre-Quaternary Geology of Hong Kong*. Hong Kong Geological Survey, Geotechnical Engineering Office, Civil Engineering Department, The Government of the Hong Kong SAR, 181p..
- Strange, P.J., Shaw, R. & Addison, R. (1990) *Geology of Sai Kung and Clearwater Bay*. Hong Kong Geological Survey Memoir No. 4, Geotechnical Control Office, Hong Kong, 111p..
- Wai, C.C. (1986) A note on the Discovery of Fossil Wood Found in the Repulse Bay Formation Sediments at Cheung Sheung, Sai Kung, New Territories. *Geological Society Hong Kong Newsletter*, 4, 5-7.
- Williams, M.Y. (1943) The Stratigraphy and Palaeontology of Hong Kong and the New Territories. *Trans. Royal Society of Canada Third Series*, 37(IV), 93-117.
- Workman, D.R. 1991. Field Guide to the Geology of the Shoreline West of Lai Chi Chong Pier, Tolo Channel. *Geological Society of Hong Kong Newsletter*, 9, 20-33.





*Plate 1: General view of the lower end of the section. This illustration shows an apparently undeformed, well-bedded sequence dipping at a relatively shallow angle towards the east (from left to right in the Plate).*



*Plate 2: Major "fault-related" discordance, with some evidence of stacking. The volcaniclastic units in this illustration are more massive and lighter in colour. Although the beds still appear to be laterally persistent, as in Plate 1, closer inspection suggests more complex variations in stratigraphy and structure. Definitive determination of variations in the younging direction throughout the section has yet to be achieved. However, some sections appear to be inverted.*



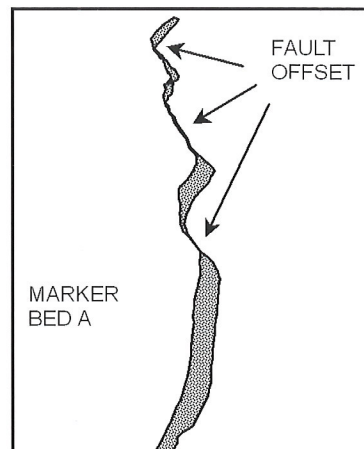


Plate 3: A close-up view of the major discordance featured in Plate 2. Spectacular offsets of a marker unit (see figure above) can be seen in this section, which confirm the sense of offset. However, the style of failure (brittle, brittle-ductile, or ductile) and the state of the marker material at the time of deformation are less clear. Material derived from the marker unit appears to have been smeared, or perhaps even flowed, along the fault plane during fault movement. In contrast, veins in the rocks suggest brittle deformation, although not necessarily at the same time as the main fault movement. The lateral extent of the discontinuous marker bed at the top of the photograph is difficult to determine, as is the control of its discontinuity.

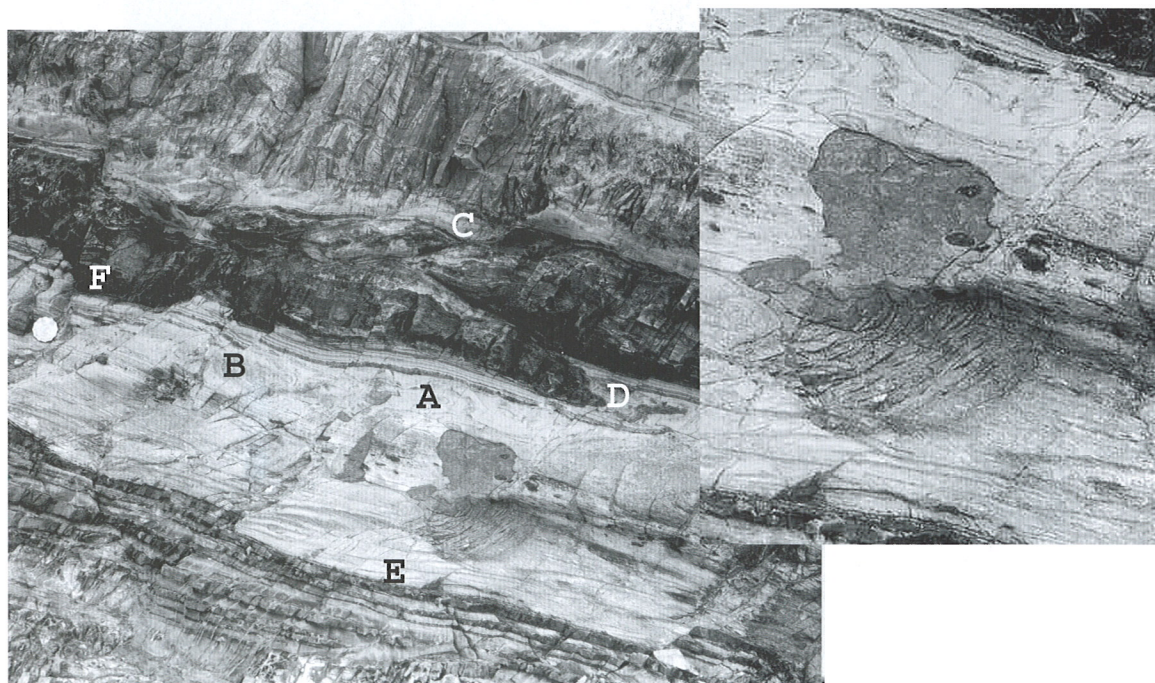


Plate 4: A close-up view of typical bedforms. This section shows laminated cherty siltstones and lighter-coloured sandstones. The sandstones exhibit a range of sedimentary depositional features including: A. Convolute laminations (see enlargement); B. Deformation styles including a range of brittle offsets, and folded and sheared beds; C. Extension (normal faulting), and D. Compression (minor thrusting), in adjacent beds; E. A minor graben structure. It is important to realize that not all of the colour variation (here shown as a grey-scale) relates to primary depositional processes. Much of it may indeed be secondary, weathering-related staining. Also, there are clearly some features (such as C and D) that provide seemingly contradictory indications of deformation mechanisms.



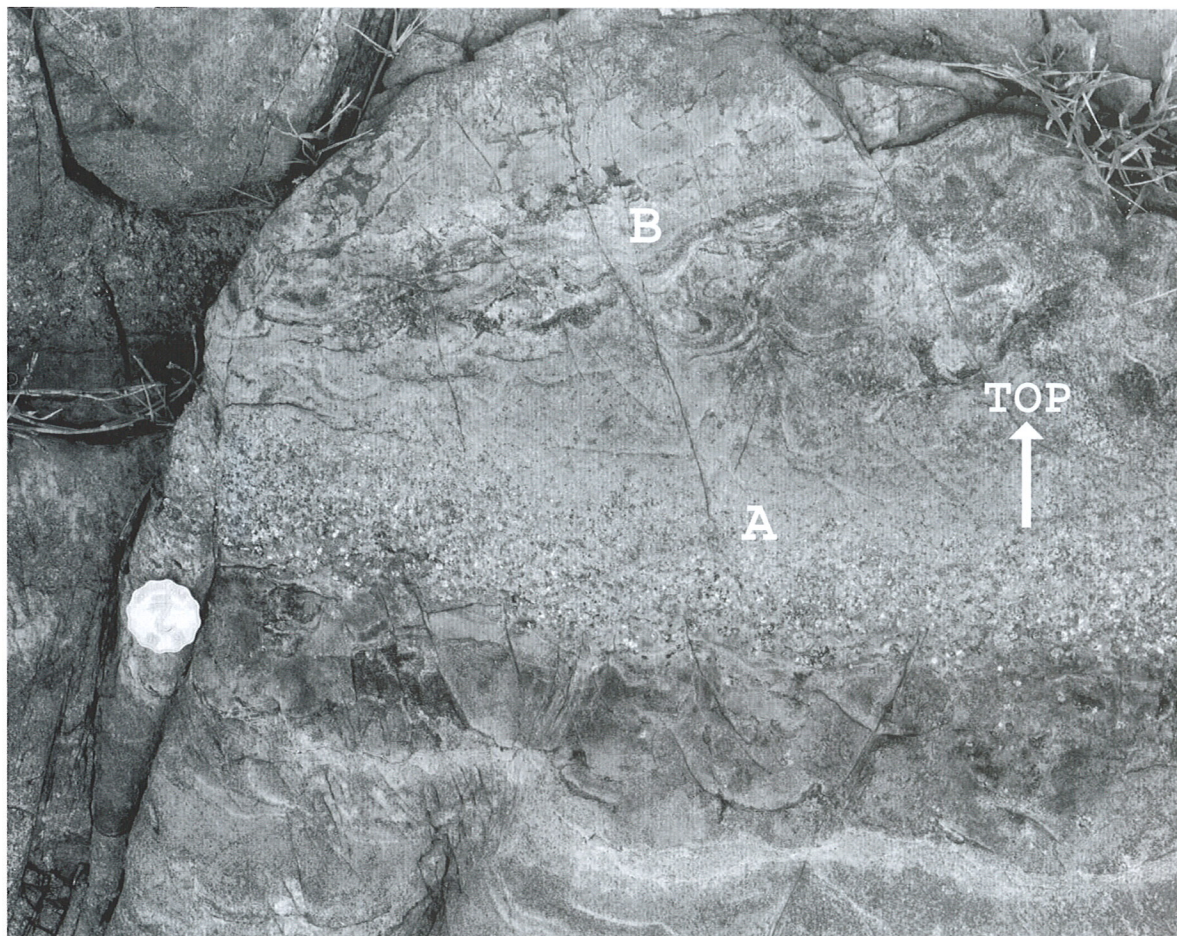


Plate 5: Primary depositional features. This illustration shows: A. Normal grading; B. Convolute bedding. The section displays elements of an incomplete Bouma Sequence (Bouma, 1962), because the sequence lacks the parallel laminated middle unit (Unit C of the Bouma Sequence). Also, the base is irregular, and does not appear to have the requisite sharp, eroded contact. Overall, the evidence suggests that this unit is a relatively proximal deposit. Elsewhere in the section, thinner, finely laminated siltstone and mudstone units may be more distal turbidites.

The environment of deposition was probably a lake in a volcanoclastic region. Thus, it is envisaged that coarse volcanoclastic material built up around the margins of the lake, washed in from the surrounding volcanic ash sheets. These accumulations would then have been periodically remobilised, possibly following seismic activity during eruptions of nearby volcanoes. Depending upon both the magnitude of the seismic event, and the amount of sediment build-up, the material would have been redistributed by turbidity currents in the lake.

There exists the possibility, although firm evidence is lacking, that some of the section may contain tuff ring deposits. Tuff ring deposits are concentric rings of volcanic ash that accumulate around a subaqueous (in this case sub-lacustrine) parasitic cone within a crater (caldera) lake. A contemporary analogue can be observed at Lake Taal in the Philippines. Associated with this form of activity are lateral volcanic surges that flow over the surface of the lake. As the surge clouds lose momentum and become depositional, the red hot volcanic ash and lapilli fall down through the cooler water of the lake. Although these features have not been certainly identified, the possibility of their existence should be borne in mind when examining the section.





Plate 6: Load and flame structures (I). This section shows asymmetrical flame structures (see the highlighted bedding contact), the asymmetry being generally from left to right, looking down dip towards the east. However, in some instances they are more complex. The complexity suggests movement, during deposition of the unit, from north to south (downslope?). The overlying unit is normally-graded, passing into parallel-laminated siltstone and sandstone units, with an increasing amount of dark grey siltstone upwards.

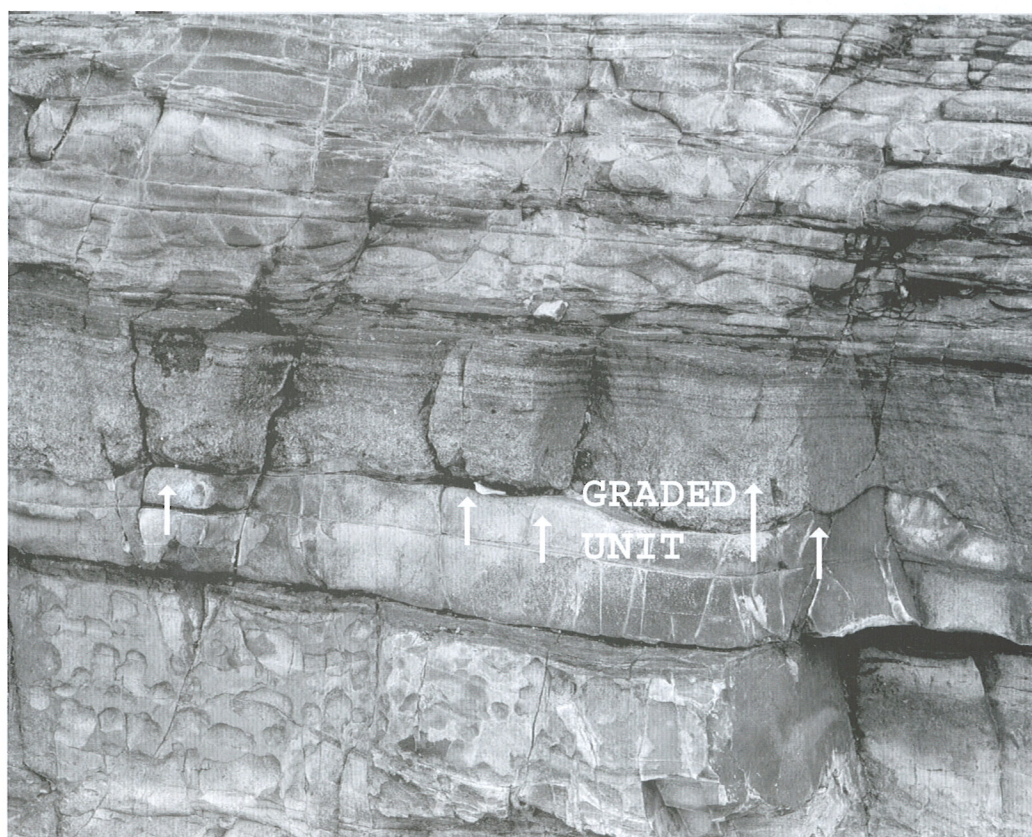


Plate 7: Load and flame structures (II). This section illustrates the same features as Plate 6. Note particularly the flame structures (arrowed on the Plate) and rafts of siltstone, the latter representing intraformational rip-up clasts or detached flames. Possible dish (dewatering) structures at the top of the exposure would indicate dessication, cracking and curling of the surface sediments, either following (possibly seasonal) lake lowering and consequent subaerial exposure, or possibly even by subaqueous processes.



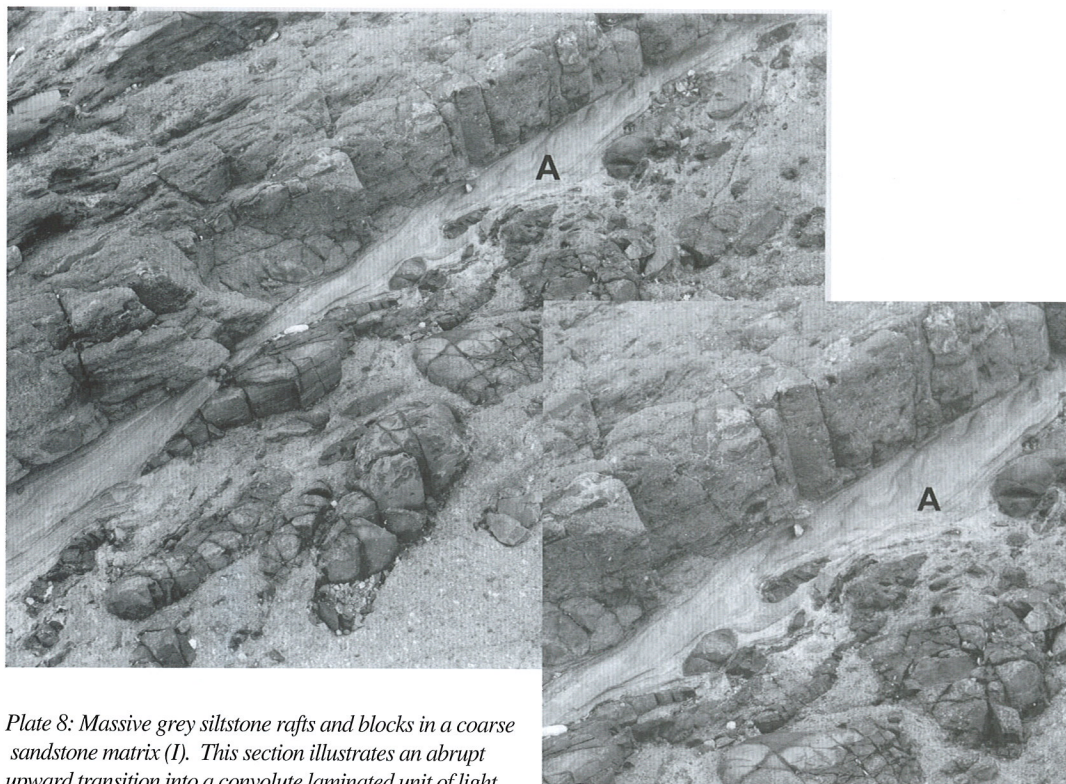


Plate 8: Massive grey siltstone rafts and blocks in a coarse sandstone matrix (I). This section illustrates an abrupt upward transition into a convolute laminated unit of light coloured siltstone/fine-grained sandstone. On the enlargement, the asymmetry of the flame structures is in the same sense as that in Plate 6, from left to right looking down dip, indicating movement (probably downslope) from north to south.



Plate 9: Massive grey siltstone rafts and blocks in a coarse sandstone matrix (II). An illustration of similar features to Plate 8. Note the asymmetry of the silt flames within the light-coloured fine-grained sandstones. It is interesting to speculate at what stage the flames developed, because they appear to pass through otherwise laterally continuous parallel lamination in the sandstones.



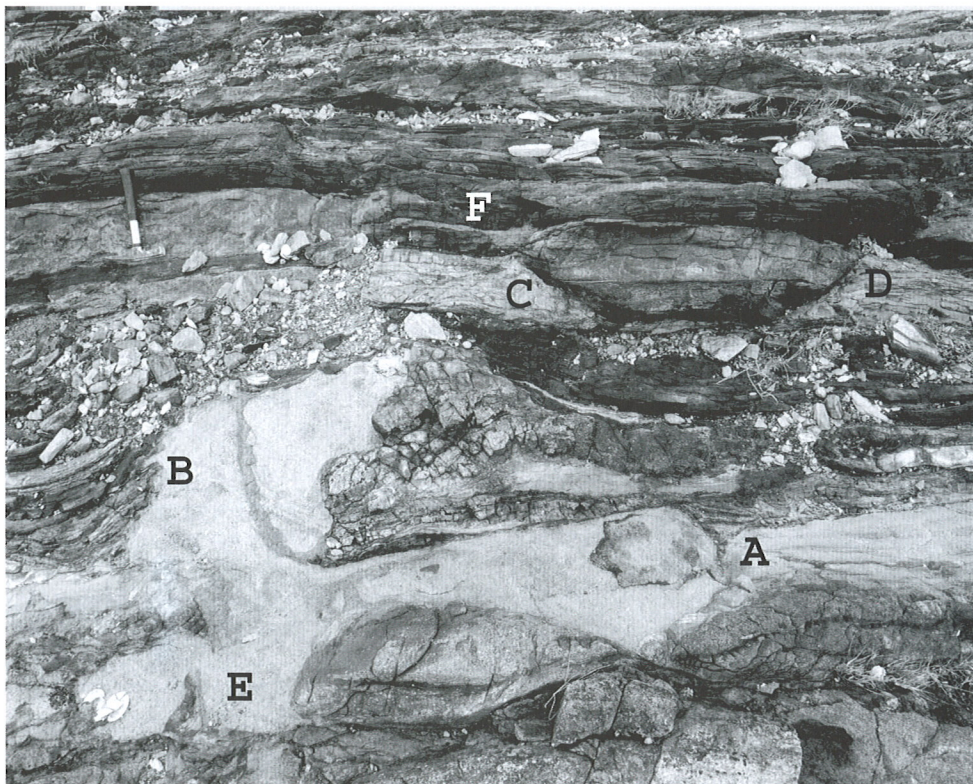


Plate 10: Exotic flames. This unit shows the migration, in various directions, of light-coloured fine-grained sandstone into the darker grey, well-bedded siltstones. Also visible are some flames of siltstone within sandstone: A. This bed appears to be the right way up, although it could be inverted; B. Protrusions along upturned bedding planes. However, the way-up is difficult to determine; C., D. and E. Three of the many examples of an extreme lack of lateral continuity in some units; F. Upwarps and bedding protrusions.



Plate 11: Major structure. This exposure demonstrates evidence of lateral stacking and bed-parallel shortening from left to right looking down dip.





Plate 12: Open folding.

*This Plate, and the following Plates 13 and 14, illustrate an increased tightening of folds, which is characteristically expressed as conjugate, typically open S-folds and tight Z-folds looking down dip and dip plunge. The intraformational nature of the folding is apparent in the top centre of the plate, where generally undisturbed bedding in the overlying sequence is apparent.*



Plate 13: Tight folding

*An illustration of a virtually recumbent fold overlain by generally undisturbed bedding, which again indicates the intraformational nature of the deformation. Hence, this suggests that the folding is a manifestation of soft sediment deformation and slumping on a mesoscopic scale. The folding can be described as a combination of an open S-fold and a very tight Z-fold. The plunge orientations of the folds are similar to the strike directions of the two dominant faults and two dominant joint sets at Lai Chi Chong.*

*Where the Z-folds become very tight, shear failure is evident, resulting in thrust development and stacking. Workman (1991) suggested that there was no pattern to the folding. However, it appears that the intraformational folding does display some internal consistency, with tight Z-folds being southerly verging. This can be interpreted in terms of slumping on a southerly directed palaeoslope.*





*Plate 14: Extreme folding. An illustration of an extreme form of the folding shown in Plates 12 and 13. This complex fold, unusually for the section as a whole, exhibits a very shallow plunge to the north. The mode of genesis of the fold is very uncertain but may be a manifestation of slumping.*



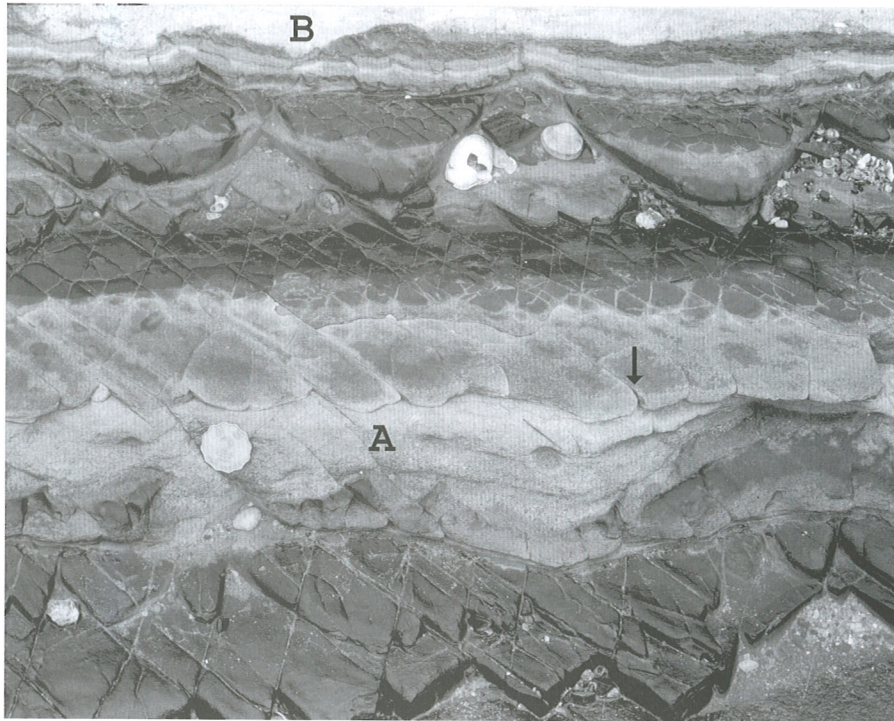


Plate 15: Spectacular asymmetrical flames. A further example of multiple flame structure development. Flames of grey siltstone protrude into the lighter coloured sandstone. The flame structures again show left to right asymmetry looking down dip, suggesting a southerly directed palaeoslope. The light-coloured sandstone unit also shows normal grading that, together with the flame structures, confirms that the exposure is the right way up. Note also in this illustration: A. Small-scale faults that appear to be similar to joints in the siltstone units, but which in the light-coloured unit are clearly displaced contacts. Close inspection of the sandstone/siltstone contact reveals that the sandstone appears to inject into some of the faults to produce flame-like structures; B. Flame and load structures in the upper part of B. Note also how alteration has pervaded the joints.

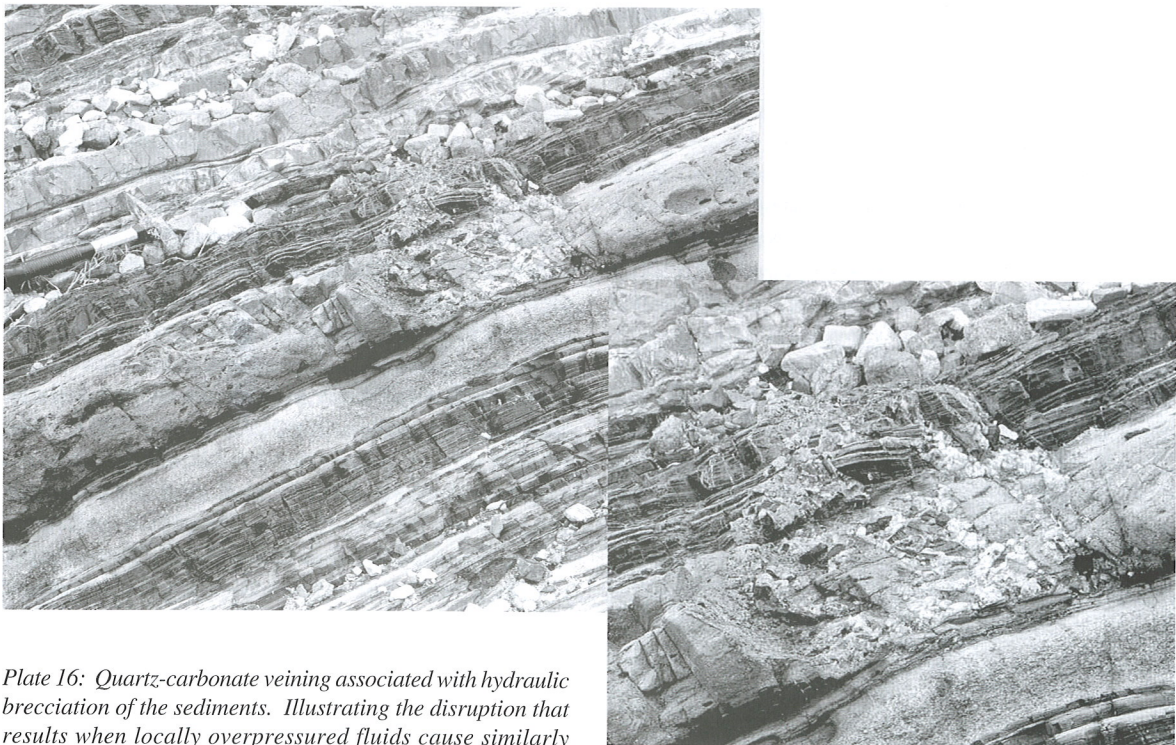


Plate 16: Quartz-carbonate veining associated with hydraulic brecciation of the sediments. Illustrating the disruption that results when locally overpressured fluids cause similarly localized deformation and/or brecciation of overlying units. The enlargement shows the feature in more detail.

## Hong Kong's Classic Geology, No. 3

### Rain Erosion: piping, rilling and gullying

Sai L. Ng & Kin C. Lam

*Geography Department, The Chinese University of Hong Kong, Shatin, New Territories, Hong Kong*

#### Introduction

Steep slopes are an integral component of the physical landforms found in Hong Kong. They make up the bulk of the land and also display a variety of forms and features that contrast with their lowland counterparts. Many slopes clearly show evidence of rain erosion (So, 1984). Rills and gullies with steep to vertical walls, and widespread badlands, are especially well-developed in Tai Lam Chung and on the small hills to the west of Castle Peak. Shallow stripping of surface soil occurs as a result of sheet erosion, especially on the hillslopes of eastern Lantau. Subsurface pipes often emerge at cutslopes.

The impact of rain erosion is significant in both aesthetic and economic terms. Rills and gullies often constitute eyesores. The removal of subsurface material may undermine the stability of slopes. Eroded materials may partially fill reservoirs, bury arable lands, roads and structures.

#### Splash erosion and sheet wash

Hong Kong experiences a subtropical monsoon climate with a mean temperature of 23°C and an annual rainfall of approximately 2200 mm (Hong Kong Observatory, 2001). Under the influence of the seasonally hot and humid climate, intensive and deep weathering has resulted in the formation of a thick regolith of weathered material over much of the territory. These areas are particularly prone to erosion.

Rainwater is an effective erosional agent. When raindrops hit the ground, the dissipation of kinetic energy can break soil aggregates and splash grains into the air. On a perfectly level plane surface, displaced soil particles are evenly redistributed. On an incline, particles tend to move downslope, with net movement being directly proportional to the slope angle.

Not all rainwater can percolate downwards immediately and so forms a surface layer of water. When this water layer has a thickness greater than about three times the diameter of the impacting raindrops, it can effectively protect soil aggregates from being broken by rain splash (Selby, 1985). However, the downward movement of a water layer over a slope can transport loose soil particles by rolling them along the ground. This form of erosion is referred to as sheet wash. The competence and capacity of the sheet wash is a function of the depth of flow, the roughness of the ground, the roughness of the particles, and the topography of the slope (Selby, 1985; Lam, 1977). Sheet wash ceases either when the

depth of flow falls below a critical value, or all of the available surface material has been removed (Selby, 1985).

Although sheet wash is usually unable to move large particles such as pebbles, it is effective in transporting clay and fine silt. While the surface fine particles are washed away, a lag or armour of large grains is often left behind (Tschang, 1972). On some occasions, earth pillars may be left standing. These consist of a column of loose materials crowned by a protective cap (Plate 1).



Plate 1 - Earth pillars on a granitic slope.

#### Piping

Rainwater and groundwater percolates both vertically and downslope through the regolith. As it does so it readily dissolves the soluble materials and displaces fine grains so that subsurface soil pipes are developed. The formation of subsurface soil pipes depends on the permeability or voidage of the soil or weathered material. One common form of voidage are gaps that appear around boulders in soil, or corestones in weathered profiles (Plate 2), especially those associated with granites and granodiorites (Crouch, 1976). These gaps initially may be only a few mm in width, but can be enlarged to as much as 2m (Nash & Dale, 1984). The flow of groundwater around the boulders is almost certainly the cause of the formation of these voids as water simply follows the line of least flow resistance. Eventually a preferred flow path will form. The movement of water through pipes may also cause them to silt up. Once this happens new flow paths must form.

Relic joints and their intersections also control the development of subsurface pipes. Piping is accompanied by removal of weathered material from the joint plane through dispersion, slaking or abrasion (Jones, 1981). Eventually, a complex 3-dimensional network of





Plate 2 - Pipe development. A pipe has formed along a gap between the soil and boulder; an opening is visible near the bottom center.

subterranean conduits of some considerable length develops. This is difficult to observe as it is only in two dimensions that they can be examined (Nash & Dale, 1984).

The most common examples of piping observed in Hong Kong are found in the top 1-2 m of the soil profile. These often occur at a textural or permeability boundary (Nash & Dale, 1984). Granitic soils and those containing numerous boulders or gravel bands are most susceptible to shallow piping because of their relatively high permeability. Shallow pipes are generally small (< 100 mm) in diameter and may be responsible for feeding deeper pipe networks. Occasionally subsurface pipes are enlarged to such an extent that collapse of the overlying material occurs, resulting in deep rills and gullies (Selby, 1985).

### Rilling and gullying

Rills may develop where surface water is diverted around objects or becomes concentrated in troughs or cracks on the soil surface. The water in a rill has sufficient depth for turbulence to develop. Consequently, rill flows can entrain even larger particles than sheet flows. In Hong Kong, the head of a rill may extend all the way to the top of a barren slope because sudden summer storms can generate sufficient flow to produce entrainment within a short distance. Individual rills can coalesce into a branching network as the divides between rills are broken down, and the water from one rill flows into a neighbour. This tends to result in rills become more widely spaced downslope (Plate 3). Rills can also widen and deepen into gullies. In terms of size, gullies are usually more than about 0.5 m in depth and width, and may be more than 10 m in length (Selby, 1985).

In Hong Kong, the formation of rills and gullies is accelerated by alternate wetting and drying of unvegetated soils (Woo, 1967). During days with no rainfall, evaporation dries soil and opens cracks. When



Plate 3 - A rill network developed on a granitic slope.

violent rainstorms develop, water on the surface cannot infiltrate immediately and is concentrated in these cracks. The resulting water torrents cause rapid erosion and incision to form rills and gullies. The rate of erosion is dependent on the amount as well as the intensity of the rainfall.

In Hong Kong, most gullies are found on slopes at angles of 10-40°. There is a close association with areas of deep weathering, especially over granitic rocks (Ruxton & Berry, 1957). The gullies usually expand in three directions. Incision lowers the gully floor. Widening occurs through lateral erosion and headward erosion extends the gully upslope. Flowing water contributes to erosion in all these directions. Lateral and headward erosion may be reinforced by mass-wasting. When the headwall and sidewalls of the gullies have been undercut, slumping may occur. Gullies seldom lengthen in their lower courses, where the presence of vegetation cover often succeeds in checking the force of running water.

Gullies may occur in a variety of shapes. Younger gullies or rills are mostly narrow and V-shaped. Later, they are readily widened through lateral erosion and mass



Plate 4 - A mature U-shaped gully on a granitic slope.

wasting. Deposits of mass wasting tend to accumulate on the gully floor transforming their cross sections into a U-shaped profile (Plate 4). Locally, whirlpools may form and scoop small pot holes (Woo, 1967).

Gullies exhibit a range of drainage patterns that may be grouped into four main types: 1. dendritic (tributary gullies meet the main gully at an oblique angle); 2. corolla-shaped (the gully head undergoes rapid widening to form a large corolla-like depression); 3. parallel (gullies run parallel to one another); 4. fan-shaped (gullies spread out like the ribs of a fan) (Woo, 1967).

## Badlands

Badlands consist of barren land surfaces caused by extensive gully erosion (Plate 5). In Hong Kong, most badlands are developed on granitic slopes, reflecting the importance of rock type in controlling the depth of chemical weathering (So, 1984). Nevertheless, human destruction of the vegetation cover for fuel and wood is of major importance (Tsang, 1964).

The gullies sometimes occur along the crests of spurs, but most are lateral gullies that cut into the valley sides. This suggests that the badland development may have involved rainsplash and sheetwash processes, with erosion starting at the spurs and extending down to the valley floor. Other active processes include eluviation that has removed material from the soil profile and slumping, which has contributed to the formation of the steep to vertical sidewalls (Grant, 1968).

The development of badlands may involve three stages (Woo, 1967). In the early "youthful" stage, the exposed mantle dries and contracts, causing surface cracks to form. The removal of fine particles then causes a coarsening of the surficial layers of the soil profile, which in turn inhibits the regeneration of vegetation. In areas subject to drier conditions, fragments of rock and soil roll downhill and may accumulate at the footslope to form terracettes. When infiltration is exceeded by the rate of rainfall, surface water begins to accumulate. Sheetwash and subsurface eluviation, cause desiccation cracks to expand into horseshoe depressions that characterise the youthful stage of development. During the second stage, underlying soil is exposed and all types of surface and subsurface erosion accelerate. Finally, in the mature stage, mass wasting strips away the cover of soil, with remnant patches being held together by remnant vegetation (Woo, 1967). In this mature stage, gullies are numerous and have been so widened and deepened that the area may be described as badland.

An effective way of controlling gully erosion and badland formation is to assist plant communities to recover. Vegetation will bind soil, improve infiltration, and reduce the surface water flow velocity. In some cases, it is necessary to build a dam of brushwood, to use netting or permeable rock to trap sediment (Selby, 1985; Woo *et al.*, 1997).



Plate 5 - Badlands at Tai Lam Chung.

## References

- Crouch, R.J. (1976) Field tunnel erosion - a review. *J. Soil Conservation Service, New South Wales*, 32, 98-111.
- Grant, C.J. (1968) Gullying and erosion characteristics of Hong Kong soils. *Proceedings of the Symposium on Recent Advances in Tropical Ecology*, 1, 94-107.
- Hong Kong Observatory Webpage (2001): <http://www.info.gov.hk/hko/>
- Jones, J.A.A. (1981) The Nature of Soil Piping- A Review of Research. *B.G.R.G. Research Monograph 3*, Geo Books, Norwich.
- Lam, K.C. (1977) Patterns and rates of slopewash on the badlands of Hong Kong. *Earth Surface Processes*, 2, 319-332.
- Nash, J.M. and Dale, M.J. (1984) Geology and hydrogeology of natural tunnel erosion in superficial deposits in Hong Kong. In: W.W.S. Yim (Ed.), *Geology of Surficial Deposits in Hong Kong*. Geological Society of Hong Kong. Bulletin No. 1.
- Ruxton, B.P. and Berry, L. (1957) Weathering of granite and associated erosional features in Hong Kong. *Bulletin of Geological Society of America*, 68, 1263-1292.
- Selby, M.J. (1985) *Earth's Changing Surface: An Introduction to Geomorphology*, Clarendon Press, Oxford.
- So, C.L. (1984) Landforms. In: T.N. Chiu and C.L. So (Eds.) *A Geography of Hong Kong*, Oxford University Press, Hong Kong.
- Tsang, C.S. (1964) Preliminary observations on the development of fluvial landforms in the humid south-eastern China. *Quaternaria Sinica*, 3, 57-67.
- Tschang, H.L. (1972) Geomorphological observations on rainwash forms in Hong Kong and some other humid regions of southeast Asia. *Chung Chi Journal*, Chinese University of Hong Kong, 11, 40-49.
- Woo, M.K. (1967) The weathering and erosion of granite upland in Hong Kong. *Geographical Bulletin*, 9, 9-19.
- Woo, M.K., Fang, G.X. and diCenzo, P.G. (1997) The role of vegetation in the retardation of rill erosion. *Catena*, 29, 145-159.



# GEOLOGICAL SOCIETY OF HONG KONG PUBLICATIONS

## Bulletins

- No.1 (1984) Geology of surficial deposits in Hong Kong, 177p.  
Yim WWS (Editor)
- No.2 (1985) Geological aspects of site investigation, 236p.  
McFeat-Smith I (Editor)
- No.3 (1987) The role of geology in urban planning, 601p.  
Whiteside PGD (Editor)
- No.4 (1990) Karst geology in Hong Kong, 239p.  
Langford RL, Hansen A and Shaw R (Editors)
- No.5 (1996) Seismicity in Eastern Asia,  
Owen RB, Neller RJ and Lai KW (Editors)
- No. 6 (2000) The Urban Geology of Hong Kong  
Page, A. and Reels, S.J.
- Marine Geology of Hong Kong and the Pearl River Mouth (1985), 96p.  
Whiteside PGD and Arthurton RS (Editors)
- Marine Sand and Gravel Resources of Hong Kong (1988), 221p.  
Whiteside PGD and Wragge-Morley N (Editors)

## Abstracts

- No.1 (1983) Abstracts of papers presented at the meeting on 'Geology of surficial deposits, September 1983, 79p.
- No.2 (1984) Abstracts of papers presented at the conference on 'Geological aspects of site investigation', December 1984, 50p.
- No.3 (1986) Abstracts of papers presented at the meeting on 'Sea-level changes in Hong Kong during the last 40,000 years', May 1986, 51p.
- No.4 (1986) Abstracts of papers presented at the conference on 'The role of geology in urban development', December 1986, 65p.
- No.5 (1988) Abstracts/extended abstracts of six papers presented at a meeting on 'Future sea-level rise and coastal development', April 1988, 79p.
- No.6 (1990) Abstracts of papers presented at the conference on 'Karst geology in Hong Kong', January 1990, 58p.
- No.7 (1991) Abstracts of papers presented at the international conference on 'Seismicity in eastern Asia', October 1991, 63p.
- No.8 (1992) Proceedings of a workshop organised by the Geological Society of Hong Kong and the University of Hong Kong, June 1992, 78p.

## Newsletter of the Geological Society of Hong Kong (1982-1993)

Some back issues are available.

## Hong Kong Geologist (1995+)

All issues are available.

## Prices

Non-member prices for the Bulletin and Abstracts range between HK\$30-300. Please direct inquiries to the Assistant Editor.

Subscription rates for the Hong Kong Geologist are HK\$200 (members), HK\$50 (student members) and HK\$250 (institutions).

---

## HONG KONG GEOLOGIST

---

### Articles:

- 1 Spatial Variation of Sediment Components in the Marine Deposits of Hong Kong  
*R.B. Owen*
- 14 Preliminary conceptual study on impact of land reclamation on groundwater flow and contaminant migration in Penny's Bay  
*J.J. Jiao*
- 21 Petrographical Features of Cataclasite: Evidence from the Lai Chi Kok-Tolo Channel Fault Zone, Hong Kong  
*Xiaochi Li & Frank F.S. Woo*
- 31 The Lai Chi Chong Section: A Photographic Feature  
*S.D.G. Campbell & R. Shaw*
- Hong Kong's Classic Geology, No. 3**
- 41 Rain Erosion: piping, rilling and gullying  
*Sai L. Ng & Kin C. Lam*

